Automation in Construction 126 (2021) 103674

Contents lists available at ScienceDirect

Automation in Construction

journal homepage: www.elsevier.com/locate/autcon

Neurobehavioral assessment of force feedback simulation in industrial robotic teleoperation

Qi Zhu [a], Jing Du [b,*], Yangming Shi [a], Paul Wei [c]

[a] Engineering School of Sustainable Infrastructure & Environment, University of Florida, 1949 Stadium Road 454A Weil Hall, Gainesville, FL 32611, United States of America

[b] Engineering School of Sustainable Infrastructure & Environment, University of Florida, 1949 Stadium Road 460F Weil Hall, Gainesville, FL 32611, United States of America

[c] Department of Computer and Information Science and Engineering, University of Florida, 432 Newell Dr, Gainesville, FL 32611, United States of America

ARTICLE INFO

Keywords:
Human-robot collaboration
Teleoperation
Force feedback
Virtual reality
fNIRS
Neurophysiological analysis

ABSTRACT

Telerobotic operation, i.e., a human operator to manipulate remote robotic systems at a distance, has started to gain its popularity in the construction industry. It is expected to help tackle operational challenges in dynamic construction workplaces. The success of telerobotic operation builds on the effective design of the human-robot interface to provide human operators with necessary senses about the remote workplaces, involving multimodal sensory cues, such as visual, audio and haptic feedback. Especially the force feedback design in telerobotic control interface is of central interest and is becoming the main feature of the bilateral control system for teleoperation, as it helps provide feedback about heavy physical interactions and processes in typical construction operations. Nonetheless, how force feedback simulation solutions affect the human operator's perceptional and behavioral reactions is less understood. This paper investigates the neurobehavioral performance of operators with a bilateral control system in a typical industrial valve operation experiment ($n = 21$). The experiment tested two force feedback conditions: Realistic (the system replicates the exact same feeling of the torque in valve manipulation operations) and Mediated (the simulation reduces the force on the human operator end by 50% to enable more flexible controls). The performance of the participants was evaluated via various metrics, including task performance, human performance and operational velocity uniformity. Data was collected with eye-tracking, neuroimaging (functional near-infrared spectroscopy, fNIRS), motion analysis, and NASA TLX surveys. The results indicated that the mediated force feedback in bilateral telerobotic operation helped more accurate operation, increased dual tasking, reduced cognitive load and more efficient neural functions; yet it encouraged participants to engage in more irregular actions, showing as dramatic changes in valve rotating speeds. The findings suggest that the force feedback design of telerobotic systems should be more carefully thought through to balance the advantages and disadvantages.

1. Introduction

The broadening cooperation between human and robot is a defining symbol of Industry 4.0 [1]. With the fast technological development, robotic applications have penetrated in various operational areas in the construction industry such as, turtlebots for construction site scanning [2,3], autonomous brick-laying robots [4], unmanned aerial vehicles (UAVs) for detecting the environment [5,6], humanoid robots in daily industrial operations [7] and construction robots collaborating with human workers in construction workspaces [8]. It is noted that construction operations are challenged by the open and evolving work environment, dynamic and changing workflows, and hard-to-define human-robot cooperation requirements [9,10]. In such an environment, telerobotic operation, i.e., human workers to manipulate robotic systems in complex tasks at a distance, is a promising approach to converge the advantages of both robotic systems and human agents in uncertain decision-making [11]. Unlike fully autonomous solutions that rely on robotic sensing and intelligence for automated task planning and execution [12], telerobotic operations enable human as the commander, while enhancing work performance and quality as it can scale human force and motion to achieve stronger, bigger or smaller action capabilities [13]. The teleoperation of drones and turtlebots in surveying and

* Corresponding author.
E-mail addresses: qizhu@ufl.edu (Q. Zhu), eric.du@essie.ufl.edu (J. Du), shiyangming@ufl.edu (Y. Shi), pwei1@ufl.edu (P. Wei).

https://doi.org/10.1016/j.autcon.2021.103674
Received 5 March 2020; Received in revised form 14 January 2021; Accepted 11 March 2021
Available online 20 March 2021

project controls can be recognized as typical and popular telerobotic applications in the construction industry [14].

One of the long-lasting challenges faced by telerobotic operation methods is human-robot interface design, i.e., how the feedback from the robotic system to the human operator should be designed and optimized to enable a better performance [15,16]. Human perception about the telerobotic workspace is highly affected by the created sensations on the operator's end via human-robot interface; literature has identified that perceptual modalities of human beings such as visual, auditory and haptic feedback, all play a critical role in generating a proper sense of the workspace and eventually affect the teleoperated task performance [17–19]. Especially haptics, including the feeling of force, motion and vibrations, have been proven helpful for accurately perceiving task status and physical systems with heavy motions and enabling precision operations [20–23] and become the main feature of bilateral teleoperation [11,24] However, fundamental questions regarding the relationship between haptic feedback design and human perception of the physical systems and processes remain unanswered. Understanding the impact of haptic feedback on the perception and performance of telerobotic operators sets the foundation for optimizing the feedback system design to compensate for the physical capabilities of human workers and facilitate better and safer construction operations.

As one of the efforts for understanding the human-robot force feedback interface, this paper investigates the neurobehavioral performance of telerobotic operators with a bilateral control system in a typical industrial valve operation, under two force feedback conditions: realistic and mediated. Without losing the generality, the two conditions under test represent typical telerobotic feedback design strategies. The realistic force feedback simulates physical forces of the remote robotic system in the most realistic way, such as the object weight, torch or resistance sensed by the robot [25]. While the mediated force feedback applies a force mediator (i.e., attenuator or amplifier) to the sensed forces for easier or better controls, such as amplifying the feeling of resistance in robot-assisted microsurgery [26], or attenuating the feeling of weight in heavy lifting operations [27]. The industrial facility turnaround shutdown operation (hereafter, "turnaround shutdown") was selected as the study case, i.e., an event wherein the entire plant is shut down for a short period of time for renewal [9]. This task can be too dangerous for human labors with the possible presence of radioactive and toxic materials, and can be too complex for autonomous robots to handle due to the uncertain, dynamic and evolving environment and hard to the preprogrammed tasks. As a result, it has been a popular use case for telerobotic operation [28]. A Virtual Reality (VR) experiment was performed where participants were required to teleoperate a series of valves, with two levels of force feedback (realistic and mediated). The human performance was evaluated subjectively by questionnaires and objectively by physiological data collected through eye tracking and functional near-infrared spectroscopy (fNIRS) device. The remainder of this paper will introduce the background, the research methodology and the findings.

2. Theoretical background

2.1. Remote robot controls

Literature has proposed distinct strategies for remote robotic controls. One strategy focuses on advancing autonomy or intelligence of remote robots for autonomous or semi-autonomous actions, such as adjustable autonomy [29], shared control [30], mixed initiatives [32] and safeguarded control [33]. These methods heavily rely on the spontaneous actions of the remote robots while human operators play a passive role as supervisor. Although many of these methods are effective in well-controlled environment with well-defined context (such as the lab environment), it is still difficult and inefficient for remote robot react flexibly [34] at operationally speed in complex, unpredictable, and diverse environments due to most robots' inability to comprehend non-preprogrammed conditions and processes in which they operate. To handle complex tasks in unstructured environment, another option is involving human in the loop by combing the unique cognitive skills of human operators with autonomous tools [35]. The human operator can intuitively integrate prior knowledge with dynamic observations and contextual clues to evaluate and adjust the robot's goals, making predictions and compensating for situational understanding. In this way, the human agent plays a more active role of being central to the sense-learn-control process [36,37]. Previous studies also showed that this human-robot cooperation amplifies a person's sensing and decision-making ability, as well as manipulation capability in remote tasks such as space and underwater exploration [38], rescue tasks in hazardous environments [39] and invasive surgery [40].

To achieve a successful human-robot collaboration in human-centered telerobotic operations, methods for integrating human agent's cognitive, perceptual and motor skills with the physical and cognitive assistance functions of the robotic systems need to be deliberately designed [41,42]. Human-robot interface is one of the key factors. A variety of feedback methods have been tested, including haptics, visual, and audio cues for providing the sense of presence in the remote environment (i.e., telepresence) and operational guidance [18–20]. Haptic feedback could refer to an overall sense of kinesthetic (information of forces, torques, position, velocity, etc.) and tactile (information of surface texture, friction, etc.) [43] Among the multimodal sensory feedback simulation of the remote environment, haptic feedback is proven to be the most effective method and thus receives most popularity in teleoperation such as bilateral control system. A bilateral control system is a control system for teleoperation with haptic feedback [44] and it attracts considerable interest because it transfers the haptic sense to a remote place [24]. In such a system, information as forces and velocities flows in both directions between the operator and the robot. A typical example is that the joystick detects the operator's position and motors provide backdrive forces and torques to the operator [45]. However, while most efforts have been focusing on the system design of haptic teleoperation systems [13,46,47] and the advantages of haptic feedback in telerobotic controls [42,48], there is still missing concrete evidence about how various forms of haptic interface affect the operator's mental and physical performance, in a positive or negative way. In addition, even though abstraction and reproduction methods of force sensation from the real environment bilateral control were proposed by several studies [49–51], there still lacks research exploring how the abstraction of force influences the operator's perception and behavior. This paper proposes to build up evidence for one of the most feasible teleoperation robots with bilateral control system in complex industrial construction operations, which is introduced in the next section.

2.2. Industrial mobile manipulator

The mobile manipulators (robot arms onboard a mobile robot) such as Tiago [52], Mobile Baxter [53,54], Fetch and Freight [55], which feature the capability of navigation, manipulation, and more flexible human-robot interaction, are proven to have more merits than the classic collaborative arms (cobots) and collaborative mobile robots (CMR) [56]. Mobile manipulators show great potentials for implementation in many new application areas such as space and underwater exploration, construction and services [57]. Previous researches have explored the use of mobile manipulators in hazardous or confined environments like oilfield and offshore plants to perform daily tasks of maintenance or equipment verification with teleoperation systems [58,59]. Several studies [60,61] also point that in addition to increasing efficiency and productivity, the mobile manipulator can also improve the operators' health, safety with additional environmental benefits, which are high priority for many industrial companies. Despite the apparent benefits of mobile manipulators at industrial workplaces, challenges remain to be solved such as navigation task and path planning, control, and intuitive human-robot interaction [62]. Although

topics of motion controls [63–65] and machine autonomy [66–68] have been widely discussed in the literature, how to provide a proper level of awareness of the workplace to the human operator via what kind of human-robot interfaces, have not received enough attention in this particular body of literature. As discussed earlier that haptics is a popular design factor of the human-robot interface. This is especially applicable for industrial mobile manipulator as most industrial operations involve not only the motion controls but also the force of the end-effector of arm driven by the physical processes (such as the need to feel the torque of a valve, or the weight of an object) [70]. Therefore, this paper focuses on understanding the impact of force feedback on human operators' neural and functional performance in the teleoperation of industrial mobile manipulators. The challenge relates to human performance assessment. We propose the use of multiple neurophysiological and behavioral assessment methods.

2.3. Neurophysiological analysis of human performance

Human performance builds on a complex neuropsychological process and involves a variety of functions related to the learning, comprehension, analysis and evaluation of the events of interest [71]. Evidence indicates that the presence of the robot could affect multiple cognitive functions and lead to unpredictable implications. Especially, as Nickerson [72] found, working with telerobot can significantly affect the attention patterns of workers in professional tasks. Yet literature still gives conflicting conclusions about the impacts of the collaborative robot on human cognition. Some studies show that robot can enable human agents to pay more attention to the higher level of cognitive tasks (such as planning) by automating less critical routine tasks [73], while others observed the opposite data as robots could also divide human attention and therefore, affect performance negatively [74]. As a result, it is necessary to provide additional evidence that helps fill the gap. Literature also recognizes that it is nontrivial to directly measure human cognitive activities as most of them are implicit [74].

As a solution, eye tracking and gaze analysis are often used as an indirect measure of cognitive activities [75–77]. Research [75,78,80,81] found that eye movement was a strong predictor of the attention allocation of the users by showing the concentration level on different areas of interest. Gaze movement patterns also indicate the specific decision-making styles of a person. Compared to the post questionnaires, gaze movement also features the tracking of sensitive real-time behavior of the user during an ongoing task. Therefore, the eye-tracking system was used in this study to help analyze the attention patterns of the subjects while performing the task.

Another solution to study human cognitive activities is neuroimaging. Recently, Functional near-infrared spectroscopy (fNIRS) has started to draw attention as a novel and invaluable tool to study and monitor tissue oxygenation changes in the brain non-invasively [82,83]. The attributes of fNIRS like portability, movement tolerability, and safety of use have made it particularly suitable for investigating brain function [84]. Comparing to other available neuroimaging techniques relying on neurovascular coupling such as functional magnetic resonance imaging (fMRI) [85] and positron emission tomography (PET) [86], and those based on the electromagnetic activity of the brain such as electroencephalography (EEG) [87] and magnetoencephalography (or MEG) [88], fNIRS is more robust for monitoring cortical hemodynamics during motor tasks or tasks involving walking given its advantages of low sensitivity to body movements and the systems' portability [84]. These features of fNIRS make it suitable for tracking worker's brain activities with heavy body motions during regular operations. Previous studies have proven that hemodynamic responses in the prefrontal cortex (PFC) measured by fNIRS can be used to quantify and classify mental workload [89], and is also linked to decision making [90]. Both metrics are essential factors influence workers' performance in complex tasks involving working memory, knowledge and motor skills. According to [91], motor stimuli increase the oxygenated hemoglobin and decrease the deoxygenated hemoglobin in the motor cortex, which contains the primary sensorimotor cortex (PSMC) and the premotor cortex (PMC). The activation signals from this area can be used to evaluate behaviors like movement planning, control and execution, which are related to physical operation as valve rotation. As a result, in this research, the prefrontal and motor cortex activities measured by fNIRS are used to study the mental workload of the worker during the task.

3. Teleoperation force feedback and data collection systems

3.1. Overall architecture

In order to examine human performance in bilateral teleoperation with different levels of force abstraction, we designed a virtual reality (VR) simulator based on our previous works connecting a haptic device with the simulated valve operation task [92–98]. Fig. 1 illustrates system architecture.

In this system, we simulated a remote industrial mobile manipulator equipped with a camera and force sensors, so it can provide the first-person view (FPV) and force information to the human operator. The human operator wore a VR headset to display the FPV from the remote robot. We used a force feedback device, Novint Falcon [99] to reproduce the sensed force from the virtual robot, and control the arm of the remote robot. As illustrated in Fig. 1, the teleoperation system provides three functions- virtual environment, automated force feedback controlling, and real-time data collection: (i) A complex pipe network system built in Unity3D game engine to simulate the real working environment with an update rate of 90 *Hz*, where the shutdown works require high level cognitive engagement (e.g., memory retrieval, planning and spatial cognition) and motor engagement (rotating the valves in certain rounds) (Fig. 2); (ii) A bilateral control system for teleoperation using Novint Falcon, a 3-DOF haptic device, as an input and output controller that simulates realistic physical feedback with the position sensing and force rendering rate of 1 kHz [99] (Fig. 3); and (iii) Neurobehavioral data collection system that collects eye tracking data (pupil size, and gaze position), motion trajectory, event markers and brain activity data measured by fNIRS. The following sections will provide more details of the system.

3.2. Virtual environment

To avoid the extra distractions from the environment, the virtual environment only contains a simulated workplace with four walls around a foursquare plane and pipelines (Fig. 2).

The pipelines contain connected pipes and 23 valves with the -radius of 3 *in.*, with each of them being able to interact with the Novint Falcon device. For each valve, two groups of parameters are transferred to the force feedback system through the socket. The first one includes shape, scale, and material data, which is used to calculate the static force feedbacks while the participants are touching the valves. The other one includes the real-time position and rotation angles of each valve, which are used to calculate the dynamic force required to rotate the valve. In front of each valve, a teleport spot is placed for the participant to switch and navigate in the virtual space.

As mentioned earlier, in this research, we mainly focused on the operator's physiological differences between two levels of force feedback when teleoperating the remote robot, so teleport was chosen as the navigation method as it simplified the route controlling task and minimized the influence on the operator pertaining to navigation. To incorporate the controller into the VR environment, a virtual robotic arm was designed to represent the physical controller, which can move on the zone X-Y-Z. In addition, we also designed the degrees of the virtual controller's freedom, which can be adjusted according to various working environments.

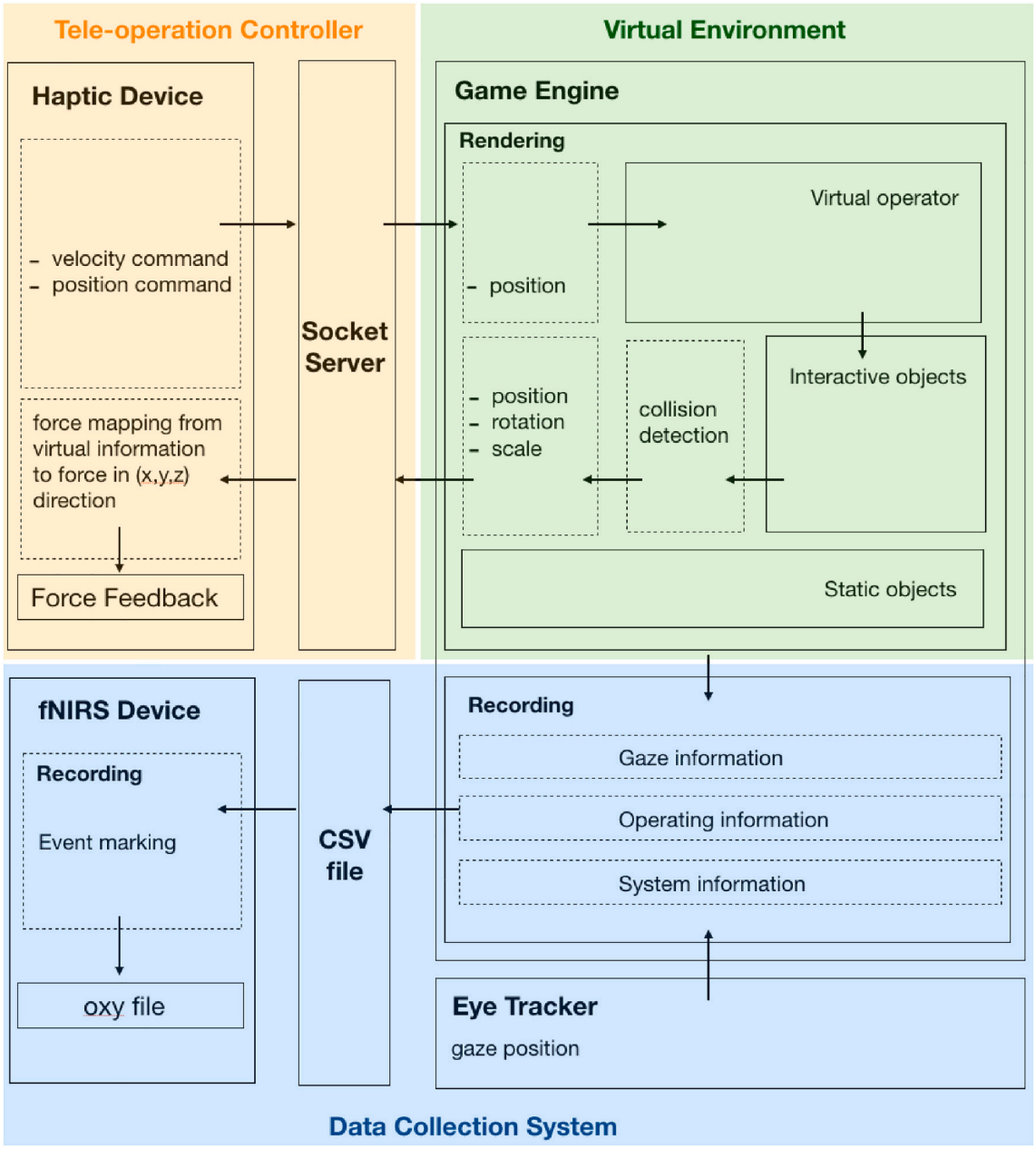

Fig. 1. Architecture of force feedback teleoperation and data collection system.

3.3. *Teleoperation controller with force feedback simulation*

We simulated physical forces in VR with Novint Falcon (Fig. 3), which has been proved stable performance in previous teleoperation research [100–102]. This device consists of three motorized arms attached to an interchangeable end-effector that communicates with Unity through the socket.

Studies on human performance in Virtual Environment (VE) show that people are generally able to detect latency as low as 10–20 ms [103], and some studies did not find performance degradations with latencies under 1 s when teleoperating the remote robot to do grasp and placement tasks [104]. In our research, all devices were wire-connected in the same room. The experiment setting was created in a direct connected manner. The lags were mainly driven by the VR device, which was under 5–10 ms and neglectable. The workspace of the Falcon is 4 *in.* in each direction. The size of the virtual workspace for each valve in the VE is also 4 *in.* in each direction. In order to make the interaction more natural and closer to real-life experience, we used one-to-one mapping of the position between the Falcon controller and the virtual representation in each direction. A physical force algorithm was applied to simulate the physical feedbacks with two modes: Realistic force feedback: the force required to spin the valve is equal to what people sense in real life (15 lbs./ft) when operating the heavy valve. Mediated –the force required to spin the valve is 50% less than the realistic force feedback case (7.5 lbs./ft); When the virtual Novint controller collides with an object in VR, a vector of force value will be updated by the algorithm that can be used as the output value for the force simulation device, and as the input for the formation exchanges of the virtual objects.

The static case of moment balance when the Novint Falcon controller touching the valve can be given with the following equation:

$$\tau = F \times R = I \times \alpha = \frac{mR^2}{2}\alpha \quad (1)$$

where τ is the magnitude of the torque or "turning effect," F is the force

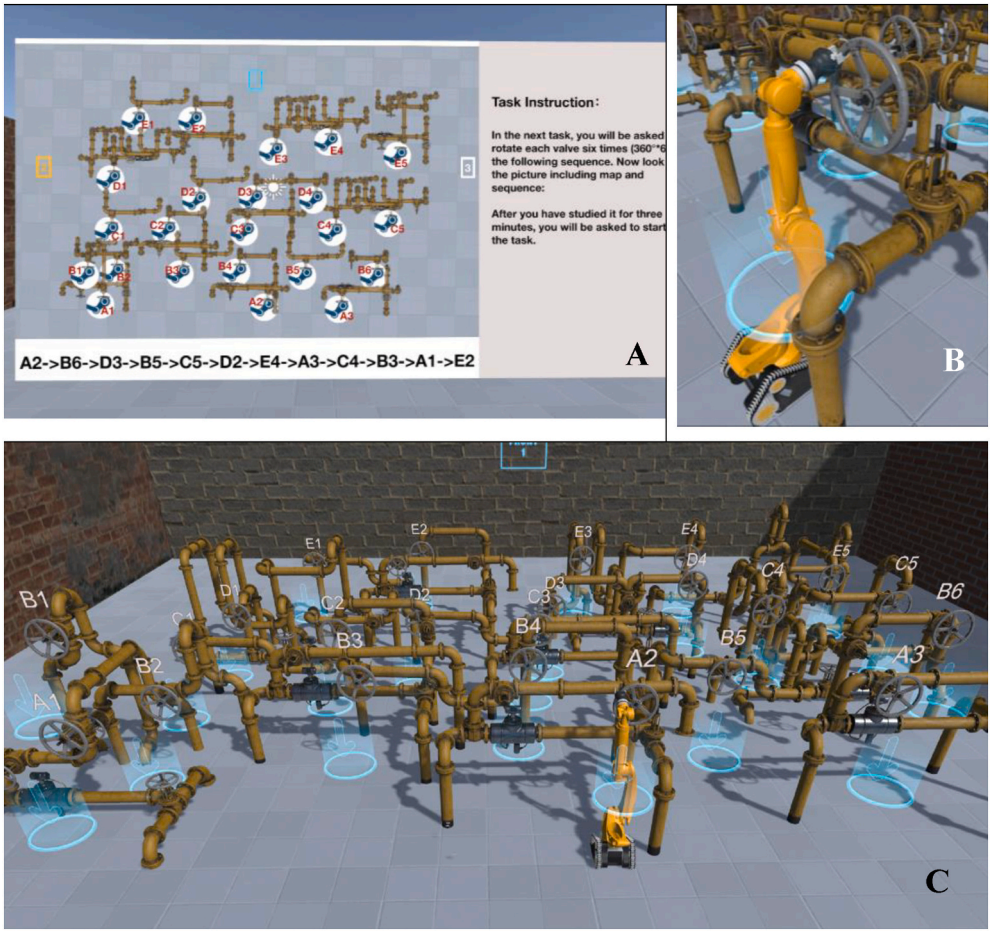

Fig. 2. The virtual environment used in the experiment. A: Instruction session; B: virtual remote robot for valve rotation; C: the complete virtual workplace.

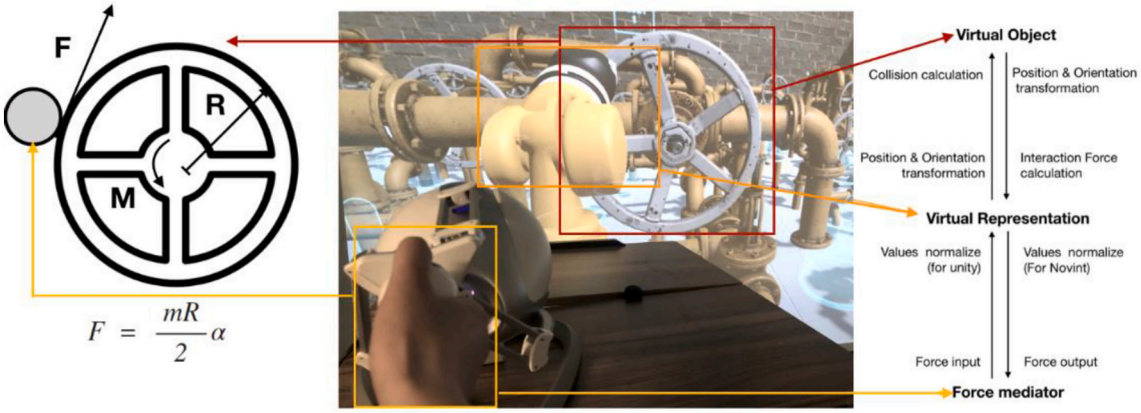

Fig. 3. Teleoperation control system with force feedback simulation.

needed to rotate the valve, R is the radius of the valve, I is the moment of inertia, m is the mass of the valve, and α is the angular acceleration. Therefore, the force provided by the Novint falcon controller can be represented as $F = \frac{mR}{2}\alpha$. By adjusting the value of the mass in our system, the controller can provide different levels of force feedback to participants.

3.4. Data collection system

In order to track participants' performance during the experiment, we used an integrated data collecting system, including build-in activity data tracking system via HTC VR device, eye tracker embedded in the HTC VIVE goggle, and brain activities tracking system fNIRS. The eye tracking device tracks gaze position and eye movement. The data can be used to analyze the participants' cognitive attention patterns. The handheld controllers were used to track motion data, including the position, rotation, and collision events. We used the motion data to analyze the participants' locations in VR, manipulating patterns, operation speed and durations. The motion tracking data can also be used to set event makers for fNIRS recording, so that the operators' actions can

be synchronized with his/her brain activities. Fig. 4 shows the experiment setup.

4. Human subject experiment

4.1. Participants

Adult participants ($n = 30$) were recruited to participate in our study. Among the 30 participants, there were 19 males and 11 females, with the mean age 23 ± 2.8 years, ranging 18–29. The fNIRS data of nine participants were excluded from the analysis due to strong noise from heavy motion artifacts as described in Section 5.1. All participants were right-handed and had no history of neurological abnormalities. Memory test (Factor-Referenced Cognitive Test, FRCT) [105] results showed that there were no significant memory performance differences among all participants.

A human-subject experiment was conducted using the VR environment to compare the remote operation performance and cognitive functions of test subjects in two conditions (Mediated and Realistic). The task involves two sessions requiring both motor and cognitive engagement of the participant. The first session was a three-minute memory session, in which the participant was required to memorize an operation workflow of twelve valves with a 2D layout map and written guidance. The following session, the remote operating task, requires both motor skills (rotating the valves) and planning (memorizing the sequence and the spatial configuration of all valves). A within-subject design was used, where each participant was exposed to two conditions: Realistic- Participants needed to rotate the valves in the right sequence and for a given number of rotations. They also needed to apply at least 2000 units of mass (15 lbs./ft) to rotate the valve; and Mediated – Participants needed only 1000 units of mass (7.5 lbs./ft) to operate the valve, given the assistance of (simulated) teleoperation system. They were asked to maintain their speed of rotation during the experiment. Fig. 4 illustrates the experiment scene and measures.

4.2. Experiment procedure

Prior to the experiment, all participants were required to complete a brief background questionnaire. This questionnaire was used to record participants' age, gender, neurological history and VR experience. Then Factor-Referenced Cognitive Test (FRCT) [105] was used to set the baseline of spatial memory ability for all participants. After each task, a NASA-TLX workload [106] questionnaire was completed for self-assessed measure including Mental Demand, Physical Demand, Temporal Demand, Performance, Effort and Frustration. The results provided a subjectively reported cross-validation to participants' mental workload and inhibitory control levels.

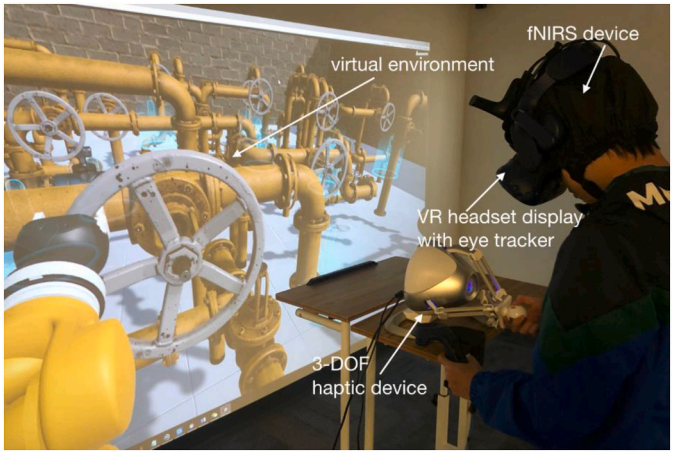

Fig. 4. Human-subject experiment setup.

Before the experiment, participants were seated and asked to adjust their hair to affixing the wireless fNIRS device. We used a wearable 24-channels fNIRS system (Oxymon, Artinis Medical Systems, Zetten, The Netherlands) to evaluate activation levels in the prefrontal cortex and motor cortex. Fig. 5 shows a schematic design of the fNIRS probes and channels used in the experiment, which contains eight detectors and ten emitters, capturing twenty-four channels for both left and right frontal lobes, including PFC and motor regions. As shown in Fig. 5, red dots indicate the sources (emitters), green dots are detectors, and blue lines are the channels. A black shower cap was used to fully cover the participant's head to ensure that the environmental light would not contaminate the fNIRS signals. Care was taken to ensure that all emitters and detectors were not affected by the VR google when the participant was wearing the VR headset. Once the fNIRS sensors, shower cap and VR device were positioned, the fNIRS devices started data collection.

Then the subject was asked to fill background questionnaires and the FRCT test before wearing the VR headset and being introduced to the experiment procedure. The experiment consisted of seven sessions (Fig. 6): (1) Training: participants were asked to finish a training session which helped them learn how to use our teleoperation system to manipulate the valve. (2) Memory session i: memorizing the operating sequence of 12 valves in 3 min. (3) Teleoperation session i: operating valves in the given sequence and for the required number of rotations (randomly in one of the two conditions). (4) Post questionnaire session i: filling NASA Task Load Index TLX to report subjective mental and user experience questionnaires. (5) Memory session ii: same requirements as review session i but with a different sequence. (6) Teleoperation session ii: same requirements as review session i but in the other force feedback condition. (7) Post questionnaire session ii. The sequence of the two performance sessions was shuffled to rule out any potential learning effects. (The demo video of this experiment can be found at https://youtu.be/cahr_-6d3zs).

4.3. Task and human performance measures

In this research, we measured task performance and human performance under the two conditions. As for task performance, the key performance metrics include task accuracy and duration. Duration was defined as the total time a participant started the teleoperation session to the point that he/she orally reported task completion. As for task accuracy, every valve was marked in two parts as shown in Fig. 7: a letter (A through E) to show its row, and a number (1 through 6) to show its specific location in the row from the left to the right. The accurate execution of the task means approaching the right valve with both the correct letter and number combination. Nonetheless, due to the excessive difficulty of the designed task, most participants failed to recall the sequence precisely. Therefore, we relaxed the criteria in the operating accuracy assessment by examining the letter and number separately. In other words, we evaluated the likelihood of a subject selecting the right row or the right location in the row separately.

As for human performance, we focused on fNIRS and eye tracking data. Specifically, for fNIRS analysis, we examined the relative activation levels of the prefrontal cortex and motor cortex under the two conditions, following the measures as described earlier. The eye tracking data was analyzed to quantify the time for planning activities and time used for motion coordination. When a participant stares at a valve, we assume that he/she is focused on motion coordination, while if the participant is looking around, then we assume that he/she is focused on planning out the next activity. With that we define dual task as when a participant looks around while still rotating the valve (i.e., performing motion coordination and planning tasks at the same time). To be noted, we also compared the rotation velocity uniformity under the two conditions, i.e., how constant the participant can keep the rotation speed when force feedback is realistic and when it is mediated. The reason is that the operation of the valves with a more uniform rotation speed is

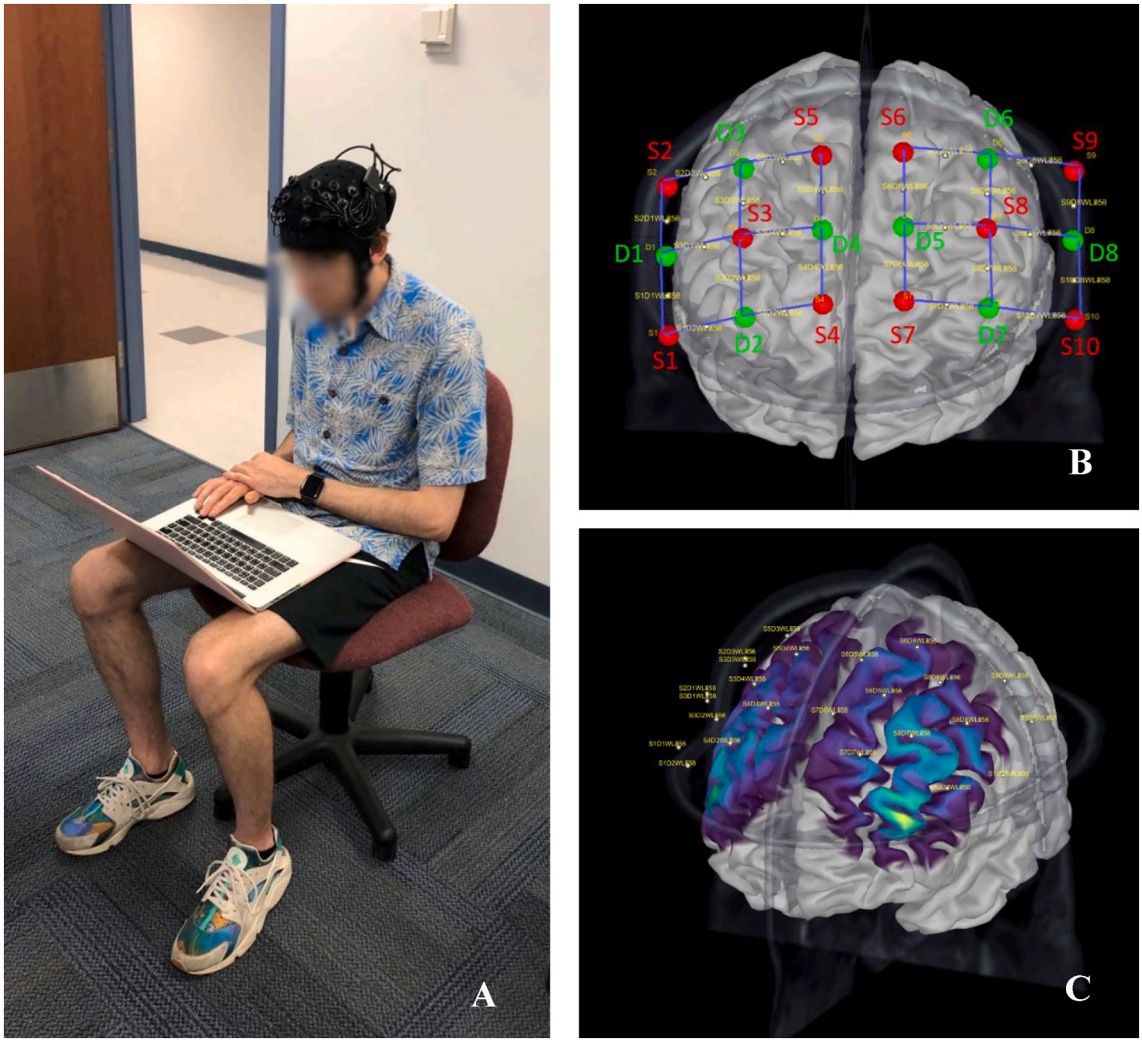

Fig. 5. fNIRS collection. A: fNIRS device to collect hemodynamic responses; B: schematic layout of fNIRS probes and channels; C: example brain activities.

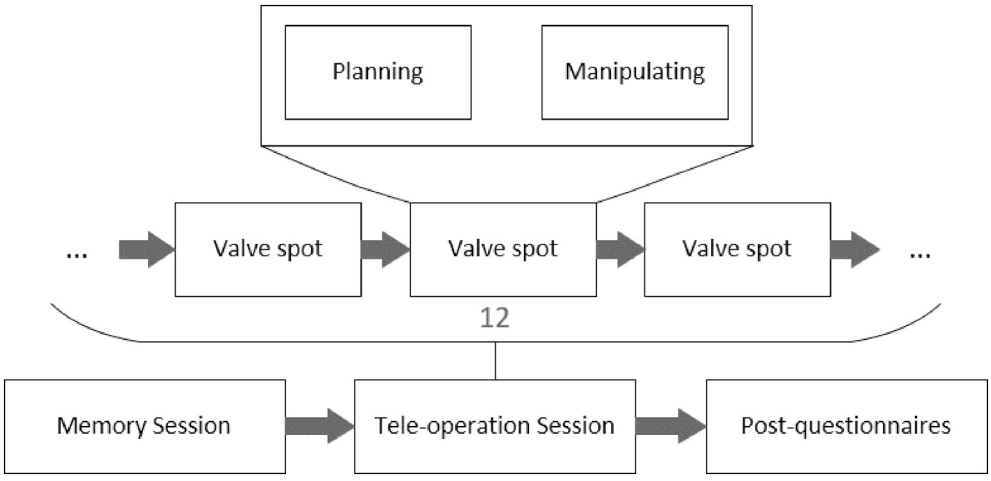

Fig. 6. The procedure of the experimental tasks under each condition.

more favorable for minimized impact on the facility. Table 1 lists the measurement metrics:

5. Data analysis and results

5.1. Task performance

Our first analysis was interested in comparing the task performance

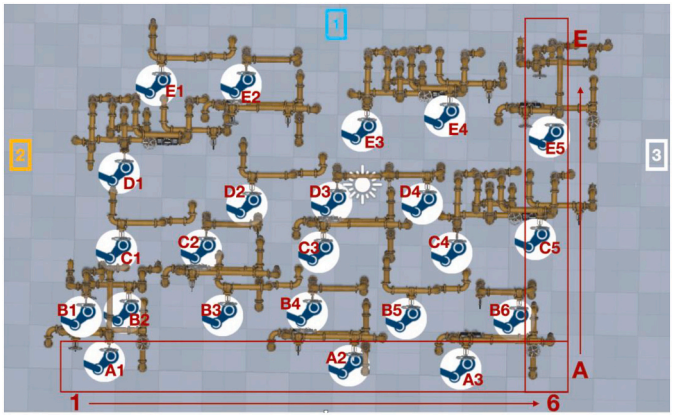

Fig. 7. The marked location of each valve in the virtual environment (The letter (A through E) was used to mark the row information from the front to the back, and the number(1 through 6) was used to mark the column information from left to right).

Table 1
The list of the measurement metrics in the experiment.

Category	Metrics	Definition	
Task Performance	Accuracy	Row (Letter)	The likelihood of the participant selecting the right row
		Column (Number)	The likelihood of the participant selecting the right location in the row
	Task duration	The total time the participant started Teleoperation session to the point that he/she orally reported task completion	
Human Performance	NASA-TXL workload	Self-assessed measure including Mental Demand, Physical Demand, Temporal Demand, Performance, Effort and Frustration.	
	MAD of prefrontal and motor cortex	Mean absolute difference (MAD) in oxygenated hemoglobin (ΔHbO2) between prefrontal and motor cortexes	
	Total ΔHbO2 consumption	The mean block change in oxygenated hemoglobin (ΔHbO2) of each channel	
	Eye tracking	Motor Action	The participant was rotating the valve with his/her gaze fixed on the valve
		Task Planning	The participant stayed at the valve location without his/her gaze fixed on the valve
		Dual Tasking	The participant was rotating the valve while looking at other areas
Operational velocity uniformity	Differential entropy(DE)	The degree of how regular and unvarying of rotation speeds was applied in the same valve, which was estimated based on Differential entropy (DE)	

under the two conditions. As discussed earlier, two performance metrics are task duration and accuracy. Shapiro-Wilk's test [92] ($p > 0.05$) was used to test the data normality and the results showed that duration and accuracy data associated with each condition (realistic and mediated) was not normally distributed. To assess whether there is a significant difference between two conditions, Wilcoxon signed-rank non-parametric test [93], a paired difference test that does not require normality, was used in our data analysis. As for task duration, the results (Table 2) indicates that the total time the subject spending on teleoperation session decrease significantly under the realistic condition ($p < 0.0001$).

As for accuracy, as shown in Table 3, the Wilcoxon signed-rank non-parametric test shown a significant increase in both row (letter) accuracy scores ($p = 0.0203$) and column (number) accuracy scores ($p = 0.0482$): Compared to realistic condition, the row accuracy in mediated condition increased from 8.36667 to 9.26667 and the column accuracy rose from 6.8 to 7.93333. Fig. 8 shows the paired analysis results for both the task duration and accuracy comparisons.

The results indicated that under the mediated force feedback condition, both task duration and accuracy were improved, suggesting additional benefits of attenuating the force feedback. The reduced time could be a result of reduced rotation time of each valve as participants were able to rotate the valves at a higher speed attributed to "lighter" resistance. We compared the summation of the saved rotation time of all valves with the total saved time as shown in Fig. 9.

It was found that the saved rotation time did not account for the total saved time between the two conditions. In addition, faster valve rotations did not explain why accuracy was improved. Another possible explanation could be that under the mediated force feedback, participants engaged in dual tasking, i.e., focusing on planning while coordinating motor activities. It allowed participants to spend more time on memory retrieval and thus the pure planning time was shortened, and memory retrieval quality was improved. To test it, we rely on eye tracking data as described in the following section.

5.2. Attention pattern

The gaze data was collected to assess attention pattern changes and implications in task performance. The gaze data, including gaze movements and fixations, were acquired using an eye tracker. Eye fixation was defined as the amount of continuous time (minimum 100 milliseconds) [107] spent looking within a 20-pixel diameter region. The total amount of time spent on fixating the valve was calculated as the sum of

Table 3
Wilcoxon signed-rank test results of dual task, row accuracy and column accuracy.

	Mean		Mean difference	Test statistic S	Prob > s
	Mediated	Realistic			
Dual Task	1977.33(1/90s)	1731.3(1/90s)	246.03(1/90s)	100.50	0.0182*
Row Accuracy	9.26667	8.36667	0.9	97.000	0.0203*
Column Accuracy	7.93333.4	6.8	1.1333	80.5	0.0482*

(Notes. *$p < 0.05$, **$p < 0.01$, ***$p < 0.001$).

Table 2
Wilcoxon signed-rank test results of Task Duration, Motor Action and Task Planning.

	Mean		Mean difference	Test statistic S	Prob < s
	Mediated	Realistic			
Task Duration	33,200.4 (1/90s)	576,792.5(1/90s)	−23,592.1(1/90s)	−229.500	<0.0001***
Motor Action	11,273.3(1/90s)	29,353.7(1/90s)	−18,080.4(1/90s)	−226.5	<0.0001***
Task Planning	23,904.4(1/90s)	29,170.1(1/90s)	−5265.7(1/90s)	−128.5	0.0030**

(Notes. *$p < 0.05$, **$p < 0.01$, ***$p < 0.001$).

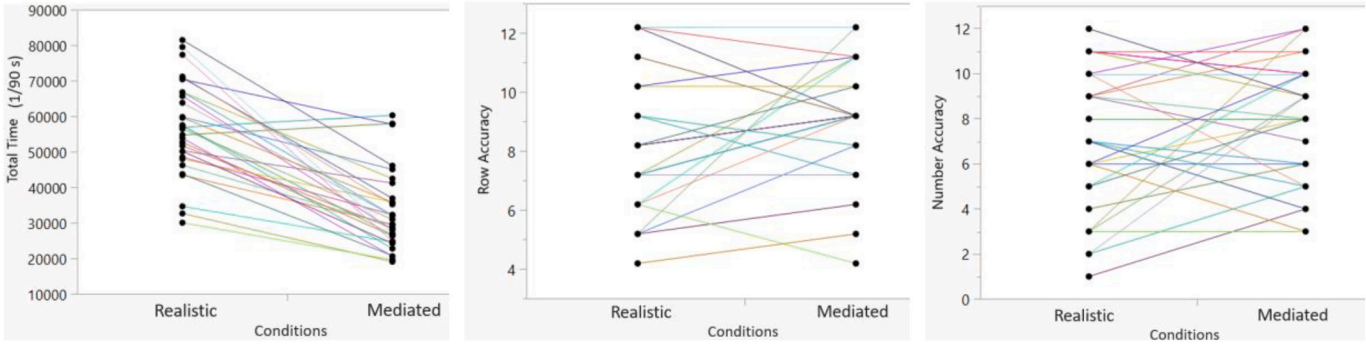

Fig. 8. The paired analysis results of the task duration, row (letter) and column (number) accuracy.

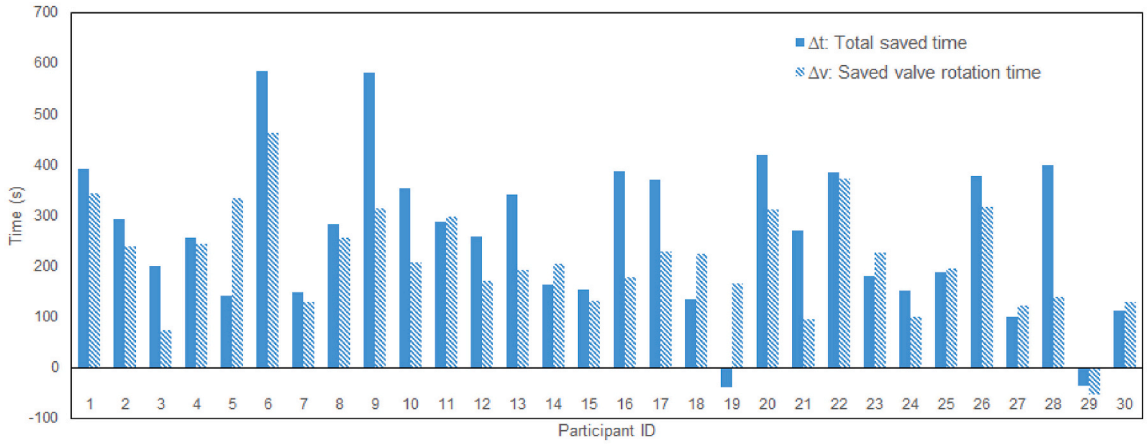

Fig. 9. Comparison of total saved time versus saved valve rotation time.

fixations within the regions of the valve. The sample rate of all the data was 90 Hz. The human motion data was also collected to provide more evidence of attention patterns, including the XYZ of the virtual robot, the rotation angle and direction of each valve. Based on gaze movement, fixations and human motion data, attention pattern was categorized into the following three classes: Motor Action - The participant was rotating the valve with his/her gaze fixed on the valve; Task Planning - The participant stayed at the valve location without his/her gaze fixed on the valve; Dual Tasking - The participant was rotating the valve while looking at other areas. These can be used to indicate if a participant completely focused on the motion coordination (rotating the valve) or engaged in dual tasking. Fig. 10 illustrates the algorithms we used to mark and calculate how much time was allocated in three of the attention pattern categories.

Shapiro-Wilk's test ($p > 0.05$) was used to test the data normality and the results showed that attention data associated with each condition (realistic and mediated) was not normally distributed. Therefore, we used non-parametric Wilcoxon signed-rank test. The Wilcoxon signed-rank non-parametric test found that there were significant differences between the two conditions in terms of the time spent on Motor Action ($p < 0.0001$), Task Planning ($p < 0.0001$) and Dual Tasking ($p = 0.0030$), as shown in Fig. 11, Table 2 and Table 3. The time participants spent in Motor Action in mediated condition decreased from 29,353.7 (326.2 s) to 11,273.3(125.3 s) compared to the realistic condition ($p < 0.0001$). Interestingly, Planning time of the mediated condition also dropped from 29,170.1(324.1 s) to 23,904.4(256.6 s) ($p = 0.003$), which deserves a further interpretation. For Dual Tasking, the mediated condition group with mean value 1699.3(18.9 s) allocated more time than the realistic group with a mean value of 825.33(9.17 s) ($p = 0.0057$).

The results, especially the one related to dual tasking, explained why total saved time was more than just the summation of saved valve rotation time (because of dual tasking), and why accuracy improved as well (more time for planning). The task performance and attention pattern analysis suggested that mediated force feedback would not only affect the motor functions of human operators, but also influenced the cognitive processes in a certain way. To obtain more direct evidence, we analyzed fNIRS data.

5.3. Total neural activation level based on fNIRS data

fNIRS data was used to provide direct evidence about how mediated force feedback and realistic force feedback in bilateral teleoperation affected the neural functions. First, fNIRS data was filtered and cleaned. For each participant, raw light intensity fNIRS data (18 optodes * 2 wavelengths per optode) were sampled at 10 Hz. For pre-processing, the signals were low-pass filtered to remove the influences from physiological changes (heartbeats, breath, Mayer waves and very low frequency oscillations(VLF) [108]. Then the motion artifacts were identified and removed through the algorithm hmrMotionArtifact from the HOMER2 NIRS processing [109] to improve signal quality. Participant data containing motion artifacts in three channels or more were removed from the analysis (9 were removed) [110]. The changes in the concentrations of oxygenated (oxy) and deoxygenated (deoxy) hemoglobin (Hb) were calculated by absorbance change of 730 and 850 nm wavelengths for each channel according to the Modified Beer-Lambert Law method [111]. The changes in oxy—Hb values were used as indicators of changes in regional cerebral blood volume as oxy-Hb(HbO2) is the more sensitive indicator of changes in cerebral blood flow (CBF) [112].

Fig. 12 shows the HbO2 signals extracted from participant 7. Different color lines are used to mark the conditions and stim events: the green lines mark the start and end of memory session and the purple

Algorithm Find the **Motor Action** , **Task Planning**, **Dual Tasking** in the record of each subject

```
function BehavioralData_in_Record(Stream)
    ▷ Motor_duration is a map where key is the valve index and the value is the operating duration
    ▷ Dual_duration is a map where key is the valve index and the value is the dual tasking duration
    ▷ Planning_duration is an integer recording the task planning duration

    for each frame in stream do

        if Operator_Collide_theValve = True then
            Moter_id ← currentValve.id
            Moter_duration[Moter_id]++                                  ▷ Operating Detection
            if Rotation_Angle = 360 then
                Moter_rotation_count[Moter_id]++
                Moter_rotation_timeStamp[Moter_id] ← currentFrame.timeStamp
            end if
            if Operator_Fixate_theValve = False then
                Dual_duration[Moter_id]++                               ▷ Dual Tasking Detection
                Planning_duration++                                     ▷ Planning Detection
            end if
        else
            Planning_duration++                                         ▷ Planning Detection
        end if
    end for
```

Fig. 10. Algorithm to find the motor action, task planning, dual tasking for each subject.

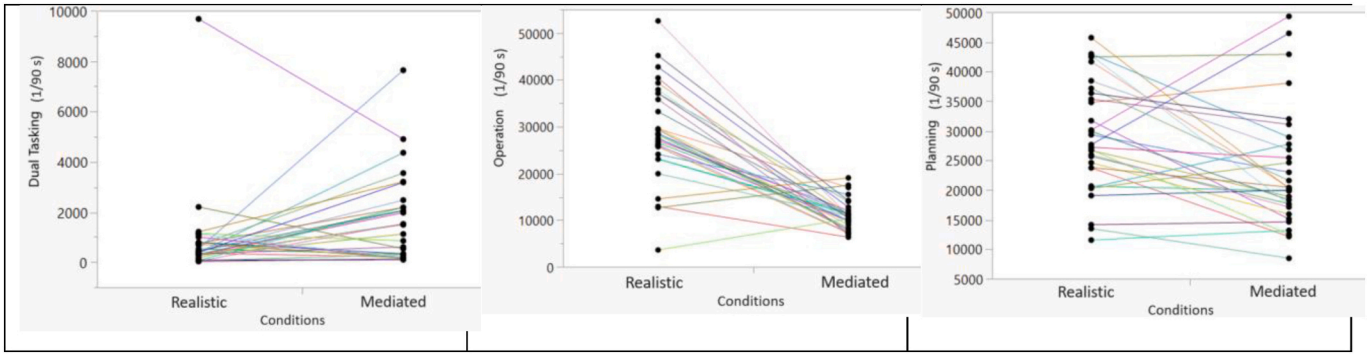

Fig. 11. The paired analysis results of the dual tasking, motor action and task planning.

lines mark the start and end of the tele-operation session in realistic condition while the yellow lines mark the same session in mediated condition. After pre-processing, the raw data was converted to HbO2 activation signals without the noise of physiological changes and motion artifacts. The differences in signal patterns pertaining to different tasks were used to compute hemodynamic trends related to varying functional activations in the two force feedback conditions.

Then fNIRS data were segmented and extracted for each marked event. For each participant's data, it was cut into three main blocks (Memory-task, teleoperation-task under Realistic condition, teleoperation-task under Mediated condition) according to the marked labels. We used the mean block changes in oxygenated hemoglobin (ΔHbO2) levels recorded from each task as the statistical feature in the analysis. The mean change in oxygenated hemoglobin has been widely used in the fNIRS research [113], which is proven to be able to capture the clear distinction between conditions. Shapiro-Wilk's test was used to test the data normality and the results showed that oxygenated hemoglobin concentration changes associated with each condition (realistic and mediated) over the prefrontal and motor cortex were not normally distributed ($p > 0.05$). Therefore, we used the non-parametric Wilcoxon signed-rank test to determine whether there were significant differences in prefrontal and motor cortex activity between the different conditions.

Our first neural analysis compared activation level changes of each of the 24 channels between the two conditions. Wilcoxon signed-rank test was used to compare averages over the 24 recording channels for both conditions. Table 4 shows the average HbO2 changes of each channel. The channels - S1D2 ($p = 0.0392$), S4D2 ($p = 0.0015$), S7D7 ($p = 0.0332$) and S10D7 ($p = 0.0074$) from PFC shows significant difference between two conditions. Compared to realistic blocks, mediated blocks were associated with a decrease in hemodynamic response. Similarly, there was also a significant decrease, in motor cortex activity when the participant was in mediated condition comparing to realistic condition,

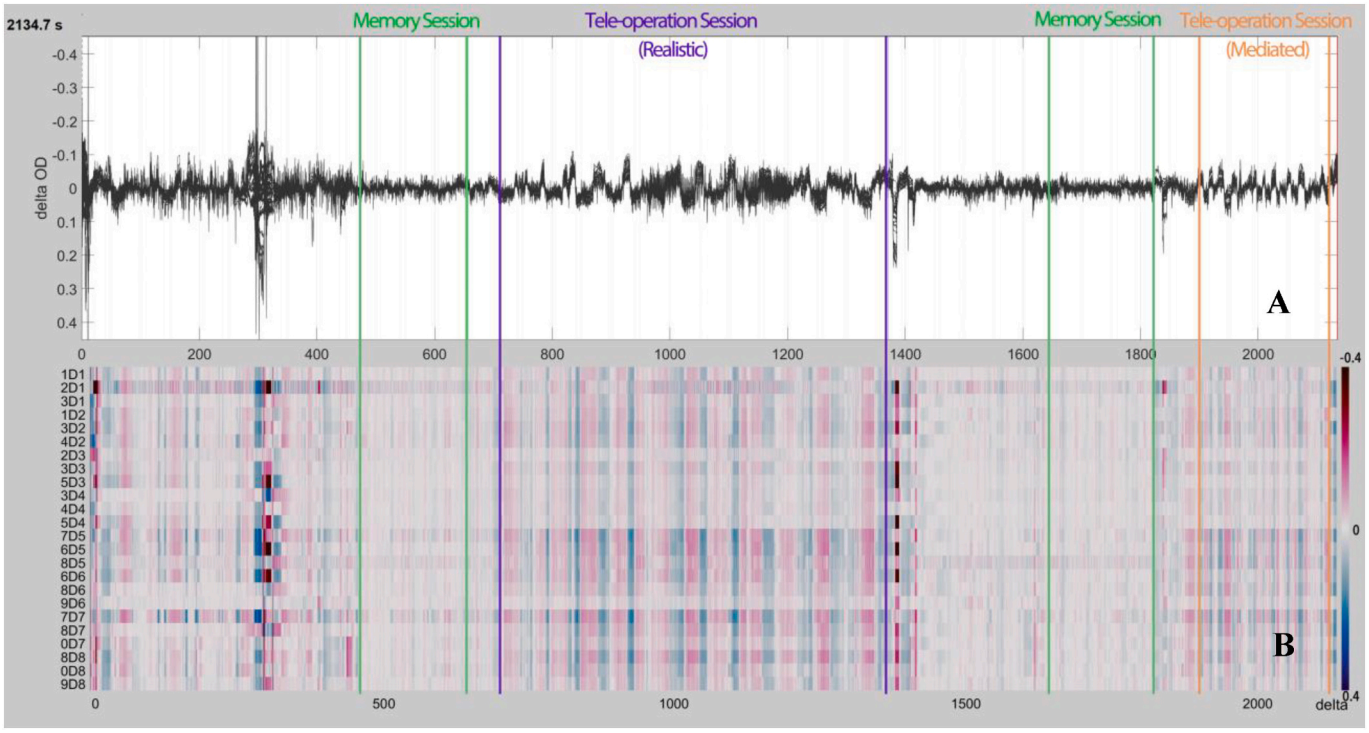

Fig. 12. Example of raw HbO2 signals of 24 channels from participant 7 during the whole experiment (A:X-aixs is time(s) and Y-axis is the ΔHbO2 levels; B: X-axis is time (s) and Y-axis is 24 channels).

Table 4
Wilcoxon signed-rank test results of 24 channels of both conditions (*$p < 0.05$, **$p < 0.01$, ***$p < 0.001$).

	Mean		Mean difference	Test statistic S	Prob < s
	Mediated	Realistic			
S1D1	−0.0001	0.00021	−0.0003	−30.500	0.1501
S1D2	−0.0004	0.00035	−0.0007	−50.500	0.0392*
S2D1	−0.0011	−0.0001	−0.0011	−59.500	0.0175*
S2D3	−0.001	3.74e-5	−0.001	−67.500	0.0074**
S3D1	−0.0004	0.00077	−0.0011	−44.500	0.0622
S3D2	0.0003	0.00146	−0.0012	−54.5000	0.0279*
S3D3	0.00188	0.00086	0.00102	12.500	0.6626
S3D4	0.00014	0.00091	−0.0008	−76.500	0.0023**
S4D2	−0.0001	0.001	−0.0011	−79.500	0.0015**
S4D4	−0.0004	0.00028	−0.0007	−65.500	0.0093**
S5D3	−0.0009	−0.0003	−0.0006	−17.500	0.2780
S5D4	−0.0013	0.0007	−0.0006	−11.500	0.3498
S6D5	−0.0006	0.00086	−0.0014	−78.500	0.0017**
S6D6	−0.001	−0.0002	−0.0008	−37.500	0.0998
S7D5	−0.0011	−1.3e-5	−0.0011	−56.500	0.0233*
S7D7	0.00016	0.0005	−0.0003	−52.500	0.0332*
S8D5	−0.0006	0.0008	−0.0014	−43.500	0.0668
S8D6	6.45e-5	−0.0013	0.00132	11.500	0.6502
S8D7	0.00171	0.00226	−0.0006	−25.500	0.1942
S8D8	−0.0011	0.00034	−0.0014	−52.500	0.0332*
S9D6	−0.0025	−0.0013	−0.0012	−84.500	0.0007**
S9D8	−0.0031	0.00073	−0.0039	−92.500	0.0001**
S10D7	−0.0005	0.00042	−0.0009	−67.500	0.0074**
S10D8	−0.0005	0.00035	−0.0009	−45.500	0.0579

from the results of channels in motor cortex – S2D1 ($p = 0.0175$),S2D3 ($p = 0.0074$), S9D6 ($p = 0.0007$), S9D8 ($p = 0.0001$).

The results indicated that the mediated force feedback in bilateral teleoperation helped reduce the brain activation levels in important functional areas related to both the motor cortex and prefrontal cortex. This could mean decreased overall cognitive load, or a simple result of the overall reduced hemodynamic reaction of the body due to less force used in the experiment. As a result, we performed NASA TLX analysis to test if participants perceived reduced cognitive load with mediated force feedback. NASA TLX was used at the end of each performance session to evaluate participants' workload levels on six different categories, including mental demand, physical demand, temporal demand, performance, effort and frustration. As shown in Table 5, each dimension of workload was analyzed separately using Wilcoxon Signed Rank test and the results indicated a significant decrease pertaining to the mental demand ($p = 0.0323$), physical demand ($p < 0.001$), temporal demand ($p = 0.0045$) and efforts ($p = 0.0005$) in mediated feedback condition comparing to realistic condition. To further test the impact on neural functions, we compared the relative engagement of prefrontal cortex versus the motor cortex.

5.4. Neural function changes based on fNIRS data

As the previous fNIRS analysis showed a significant decrease in both prefrontal and motor cortexes, we performed a neural functional analysis to examine whether there were different HbO2 activation differences between prefrontal and motor cortexes in two conditions. Due to the sensitivity to extreme values, we used mean absolute difference (MAD) instead of the absolute ratio. The MAD between the prefrontal and motor cortex was calculated as the result of block mean of channels (S9D6, S9D8) from left PFC subtract the ones from the left motor cortex

Table 5
Wilcoxon signed-rank test results of NASA-TXL workload test.

	Mean		Mean difference	Test statistic S	Prob < s
	Mediated	Realistic			
Mental	6.41176	7.17647	−0.7647	−105.50	0.0323*
Physical	2.55882	5.73529	−3.1765	−294.50	<0.0001***
Temporal	2.94118	4.14706	−1.2059	−146.00	0.0045**
Performance	5.69697	5.27273	0.42424	20.500	0.6407
Effort	6.08824	7.32353	−1.2353	−180.00	0.0005**
Frustration	4.29412	4.82353	−0.5294	−47.500	0.2106

(Notes. *$p < 0.05$, **$p < 0.01$, ***$p < 0.001$).

(S7D7, S10D7). The Wilcoxon signed-rank test was used to test whether there were differences between the MAD of each pair between PFC and motor cortex in two conditions. Table 6 and Fig. 13 shows the results of the pairs. The result shows the MAD of HbO2 changes between the left motor cortex and left PFC experienced a significant decrease in mediated condition compared to realistic condition. It shows that mediated force feedback allowed participants to engage more in prefrontal activities (planning and logic thinking) than motor action coordination. This finding supports the previous task performance and attention pattern observations about leaning to planning rather than repetitive motions under mediated force feedback.

5.5. Operational velocity uniformity

So far, all analyses seem to suggest apparent benefits of mediated force feedback (in our case, attenuated force) in bilateral teleoperation. Yet in the experiment, we observed that under the mediated condition participants tended to change the valve rotation speed dramatically (e.g., Fig. 14), possibly due to the reduced resistance and increased easiness of switching the speed. The reason we are interested in measuring the velocity uniformity of valve rotation is that evidence shows that different valve opening degrees will influence flow resistance properties and internal features of gate valve [114]. Therefore if the rotation speed of the valve changes too fast, the pipe system would also experience rapid changes and thus increase the risks for operation. The affected operational velocity uniformity of valves affects the simultaneous pressure of liquid or air flows inside the pipeline, which can further impact the long-term performance and the durability of the facility [112]. A more uniform rotation speed also helps improve the life of valves and the system [115]. As a result, for different types of valves, standards are usually given by the manufacturers to define the optimal rotation and opening speeds [116].

Therefore, we also tested velocity uniformity of the teleoperating in the valve manipulation task. The velocity uniformity of the valve manipulation is defined as the degree of how regular and unvarying of rotation speeds was applied in the same valve, which was estimated based on Differential entropy (DE) in this study. DE was used as the indicator because it measures the average surprisal of a continuous random variable that is proven to be sensitive to capture the variational information of time series data [117–119]. DE is calculated with the following equation:

$$h(X) = -\int_X f(x) log(f(x))dx \tag{2}$$

where X is a random variable with a probability density function (PDF) f (x). In our case, the data set X obeys the gamma distribution with a shape parameter α and an inverse scale parameter θ. We used formulae (2) to estimate the level of uniformity velocity of valve rotation for each participant. The analysis was performed per the following steps: 1) Average speed calculating: we calculated the duration of the participant spending for per rotation in each valve. The average speed for each rotation was represented as the total time finishing the one rotation circle in 360 degrees. 2) Gamma distribution fitting: we estimated the parameters (α and θ) of the gamma distribution that fits best to the rotation speed dataset by moment method.

Table 6
Wilcoxon signed-rank test results of MAD between left PFC and left motor cortex of both conditions.

	Mean		Mean difference	Test statistic S	Prob < s
	Mediated	Realistic			
MAD	−0.0054	−0.0015	−0.0039	−52.500	0.0332*

(Notes. *$p < 0.05$, **$p < 0.01$, ***$p < 0.001$) and the paired analysis result.

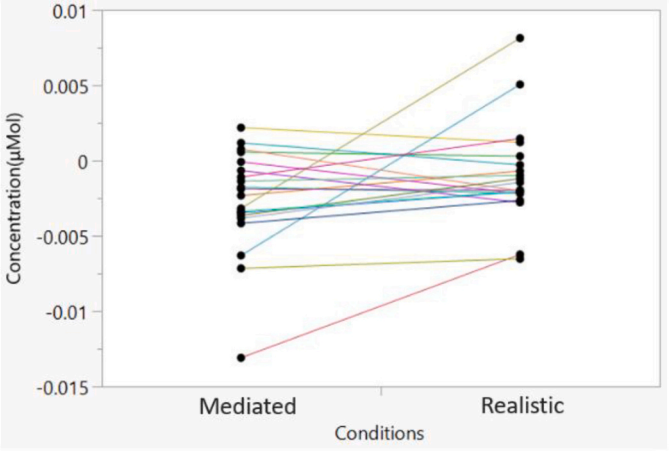

Fig. 13. The paired analysis result of MAD between left PFC and left motor cortex.

$$\widehat{\theta} = \frac{1}{n\overline{X}} \sum_{i=1}^{n} \left(X_i - \overline{X}\right)^2 \tag{3}$$

$$\widehat{\alpha} = \frac{n\overline{X}^2}{\sum_{i=1}^{n} \left(X_i - \overline{X}\right)^2} \tag{4}$$

3) DE calculating: Then the PDF was calculated with formulae (5). We calculated DE of rotation speed data of each subject in both conditions separately.

$$f(x) = \frac{1}{\Gamma(\alpha)\theta^{\alpha}} x^{\alpha-1} e^{-\frac{x}{\theta}} \tag{5}$$

4) Pair Analysis: After getting two sets (Realistic and Mediated) of DE data, we ran pair analysis by using Wilcoxon signed-rank test to compare whether there is significant difference between two conditions for each subject. As shown Table 7 and Fig. 15, the Wilcoxon Signed Rank test indicated a significant difference within two conditions. The DE in (mediated) condition is higher than (realistic) condition (Prob > S = 0.0008). The results found that under mediated force feedback, participants tended to control the remote robot to rotate the valves in a more irregular way, posing challenges to the facility.

6. Discussion

The experiment data showed significant neurobehavioral differences between the realistic and mediated force feedback conditions in the bilateral teleoperation. First, results indicated that both task duration and task accuracy were improved with mediated force feedback. It is driven by increased valve rotating speed and increased time for planning activities. Second, the gaze tracking analysis found that participants tended to engage more in dual tasking (i.e., rotating the valve while planning out the following activities) under the mediated force feedback. It further explains why the mediated force feedback helped save task execution time and improved the accuracy. Third, the fNIRS data analysis found that under mediated force feedback the overall activation level of multiple brain areas related to prefrontal and motor cortexes reduced, suggested reduced cognitive load. A NASA TLX survey supported the neural analysis findings since subjects reported reduced Mental Demand, Temporal Demand and Effort. We further tested the neural functional changes and found that under the mediated force feedback condition, the prefrontal cortex showed stronger activities compared to the motor cortex. It indicates that mediated force feedback allowed participants to engage more in planning activities than motion coordination. It supports the findings from the task performance and

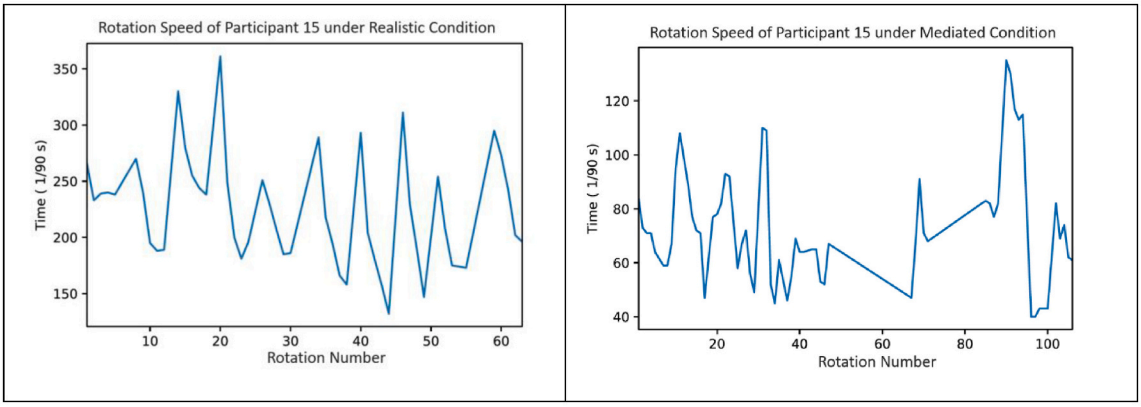

Fig. 14. Rotation speed of participant 15 under both conditions.

Table 7
Wilcoxon signed-rank test results of valve rotation speed differential entropy between conditions.

	Mean		Mean difference	Test statistic S	Prob > s
	Mediated	Realistic			
DE	0.7601	0.12021	0.63992	129.500	<0.0001***

(Notes. *$p < 0.05$, **$p < 0.01$, ***$p < 0.001$) and the paired analysis result.

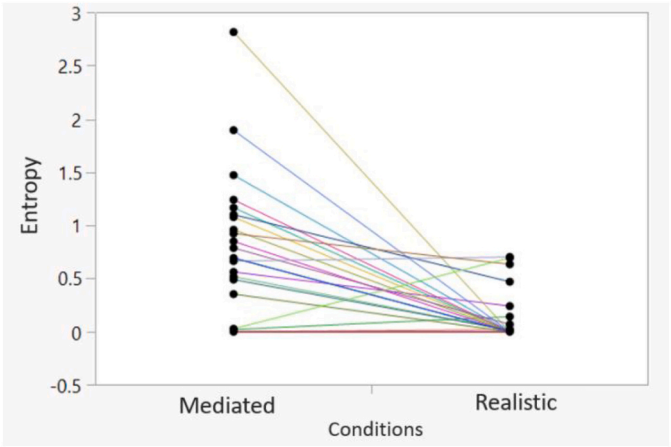

Fig. 15. The paired analysis result of valve rotation speed differential entropy between two conditions.

attention pattern analysis.

However, further analysis found that despite the various neural functional and performance benefits of using mediated force feedback in the bilateral teleoperation, it led to more irregular actions in performance. It was a possible side effect of granting more freedom for easier motion controls. The irregular actions may have a negative impact on the facility over the long term. This finding indicates that the implications of mediated force feedback may not be direct and evident. In our experiment, we found that mediated haptic feedback, i.e., reduced resistance in controls, did improve operation time and the neural performance of the operator. However, it was also found that the mediated haptic feedback also encouraged inconsistent valve rotation speeds in most participants, which would increase the risks for valve operation and affect the expected life of the valve and the facility. As a result, it may represent a fairly complex nonlinear relationship between the force feedback magnitude and human functions and performance. And it may present an opportunity for finding the optimal point for simulating force feedback from the remote robot (lower force feedback is not always beneficial) in terms of balancing the performance and operational velocity uniformity.

This study does not report the condition of zero force feedback. We found that without any force feedback, the operator's hand motion speed was always faster than speed limit of the end effector of the remote robotic system, because human hand and waist motions are naturally faster than the mechanical design limit or operational requirements of the remote robotic system. As a result, there is a perceived time delay in teleoperation. In this case, human operators start to develop substantially different behaviors to counteract the control delays, such as the "start-and-stop" strategy [120]. In other words, when force feedback = 0, the focus of the scientific investigation will be substantially different because of the induced perceptual-motor malfunction, i.e., the inability to effectively integrate perceptual information with the execution of voluntary behaviors [121–123]. Human sensorimotor control relies on multimodal sensory feedback, such as the visual, auditory, and somatosensory (tactile and proprioceptive) cues, to make sense of the consequence of the initiated action [124–126]. When perceptual ability is lacking, the motor planning and feedback loop is broken. In teleoperations, noticeable lags between motor action and feedback due to zero force feedback could create a similar mismatch in motor perception, and therefore, lead to comparable consequences of perceptual-motor dysfunction. The theoretical basis, investigation methods and scientific focuses for the two scenarios - with and without force feedback – are different. It is overwhelming to report both studies in a single paper, including different bodies of literature, different research and analysis methods, and different hypotheses. This paper focuses on testing the neural functions and performance given different force feedback discount factors in bilateral teleoperation, without any perceived time delays.

7. Conclusions

Attributed to the momentum robotic technologies in various industries, human robot collaboration has been greatly promoted and widely tested in the construction industry to facilitate traditionally challenging tasks such as environmental survey and facility operation. Among all Human-Robot Collaboration (HRC) [127] strategies, this study focuses on the bilateral telerobotic operation where a human operator remotely controls a telerobot with force feedback in a different place. This is particularly applicable to complex construction operations, such as facility maintenance, as it removes human agents from the hazardous and dangerous work environment, while still putting human in the center of task planning and decision making. The success of bilateral teleoperation builds on an effective and intuitive design of human robot interface. Especially, for tasks involving heavy motions and physical processes, the force feedback is critical to create a sense of presence and to enable better robotic controls.

In this study, we performed a VR valve manipulation experiment ($n = 21$) to test human operators' neurobehavioral performance under two conditions: realistic force feedback where the system replicates the same feeling of the force, and mediated force feedback where the simulation reduces the force on the human operator end by 50% to enable more flexible controls. The task performance, attention pattern and neural analyses all found significant benefits of mediated force feedback in bilateral teleoperation, including faster and more accurate operation, increased dual tasking, improved cognitive load status and more efficient neural functions. However, it was also found that mediate force feedback encouraged participants to engage in more irregular actions, showing as dramatic changes in valve rotating speeds. The findings suggest that force feedback design of bilateral teleoperation systems should be more carefully thought through to balance the advantages and disadvantages.

This study also demonstrated the use of VR simulation in HRC studies. Our system connects a haptic device with a simulated robotic system with Unity game engine. It should be noted that the same system can be transferred to a real robotic system, which is one of the research plans the authors are working on. The future work also includes testing the interaction effects of multiple sensory simulation – visual, audio and haptics – in telerobotic operations.

Several research limitations still need to be addressed in future work. First, this research was conducted in a well-controlled laboratory environment. Some influence factors of teleoperation, such as time delay and system stability, were controlled by the experiment setting. Even though it could help focus on the primary research scope – the human operator's perception and neurobehavioral performance under two force feedback conditions, their potential influence should be considered in the real-world environment. Furthermore, literature has shown that the bilateral control instability can be compensated by impedance control using force feedback devices [128,129]. We expect that the operator's behavioral changes under different haptic feedback conditions could be used as predictive parameters to compute the complementary stability model. Second, the control variables of this research could be enriched. Based on the findings from this study that the scaled haptic feedback affected the average valve rotation speed, adding a damper factor could help mitigate the irregularity and better examine the relationship between them. Also, adaptive attenuation is another important factor for studying haptic feedback in teleoperation. Researches have shown that it should help both compensations in time delay [130,131] and precise operations [132,133]. Adding more experiment conditions will be on our future agenda as it helps get continuous data points for varying conditions, leading to a predictive model.

Declaration of Competing Interest

The authors declare that they have no known competing financial interests or personal relationships that could have appeared to influence the work reported in this paper.

Acknowledgments

This material is supported by the National Science Foundation (NSF) under grants 1937053 and 2024784. Any opinions, findings, conclusions, or recommendations expressed in this article are those of the authors and do not reflect the views of the NSF.

References

[1] M. Rüßmann, et al., Industry 4.0: the future of productivity and growth in manufacturing industries, Boston Consul. Group 9 (1) (2015) 54–89. Available: https://www.inovasyon.gen.tr/images/Haberler/bcgperspectives_Industry40_2015.pdf.

[2] V. Vickranth, S.S.R. Bommareddy, V. Premalatha, Application of lean techniques, enterprise resource planning and artificial intelligence in construction project management, in: International Conference on Advances in Civil Engineering (ICACE-2019) 21, 2019, p. 23. Available: https://www.ijrte.org/wp-content/uploads/papers/v7i6c2/F10270476C219.pdf.

[3] K. Asadi, et al., Vision-based integrated mobile robotic system for real-time applications in construction, Autom. Constr. 96 (2018) 470–482, https://doi.org/10.1016/j.autcon.2018.10.009.

[4] M.J. Pivac, M.B. Wood, Automated Brick Laying System for Constructing a Building from a Plurality of Bricks, Google Patents, 2012. Available: https://patents.google.com/patent/US8166727B2/en.

[5] D. Roberts, T. Bretl, M. Golparvar-Fard, Detecting and classifying cranes using camera-equipped UAVs for monitoring crane-related safety hazards, in: Computing in Civil Engineering 2017, 2017, pp. 442–449, https://doi.org/10.1061/9780784480847.055.

[6] P. Kim, J. Park, Y.K. Cho, J. Kang, UAV-assisted autonomous mobile robot navigation for as-is 3D data collection and registration in cluttered environments, Autom. Constr. 106 (2019) 102918, https://doi.org/10.1016/j.autcon.2019.102918.

[7] H. Hasunuma, et al., A tele-operated humanoid robot drives a lift truck, in: Proceedings 2002 IEEE International Conference on Robotics and Automation (Cat. No. 02CH37292) 3, IEEE, 2002, pp. 2246–2252, https://doi.org/10.1109/ROBOT.2002.1013566.

[8] D. Kim, A. Goyal, A. Newell, S. Lee, J. Deng, V.R. Kamat, Semantic relation detection between construction entities to support safe human-robot collaboration in construction, in: Computing in Civil Engineering 2019: Data, Sensing, and Analytics, American Society of Civil Engineers, Reston, VA, 2019, pp. 265–272, https://doi.org/10.1061/9780784482438.034.

[9] A. Dubois, L.-E. Gadde, The construction industry as a loosely coupled system: implications for productivity and innovation, Constr. Manag. Econ. 20 (7) (2002) 621–631, https://doi.org/10.1080/01446190210163543.

[10] A. Stroupe, T. Huntsberger, A. Okon, H. Aghazarian, M. Robinson, Behavior-based multi-robot collaboration for autonomous construction tasks, in: 2005 IEEE/RSJ International Conference on Intelligent Robots and Systems, IEEE, 2005, pp. 1495–1500, https://doi.org/10.1109/IROS.2005.1545269.

[11] P.F. Hokayem, M.W. Spong, Bilateral teleoperation: An historical survey, Automatica 42 (12) (2006) 2035–2057, https://doi.org/10.1016/j.automatica.2006.06.027.

[12] G. Hitz, A. Gotovos, M.-É. Garneau, C. Pradalier, A. Krause, R.Y. Siegwart, Fully autonomous focused exploration for robotic environmental monitoring, in: 2014 IEEE International Conference on Robotics and Automation (ICRA), IEEE, 2014, pp. 2658–2664, https://doi.org/10.1109/ICRA.2014.6907240.

[13] S. Hirche, M. Buss, Human-oriented control for haptic teleoperation, Proc. IEEE 100 (3) (2012) 623–647, https://doi.org/10.1109/JPROC.2011.2175150.

[14] S. Siebert, J. Teizer, Mobile 3D mapping for surveying earthwork projects using an unmanned aerial vehicle (UAV) system, Autom. Constr. 41 (2014) 1–14, https://doi.org/10.1016/j.autcon.2014.01.004.

[15] G. Burdea, J. Zhuang, Dextrous Telerobotics with force feedback–an overview. Part 1: human factors, Robotica 9 (2) (1991) 171–178.

[16] M.A. Al-Mouhamed, M. Nazeeruddin, N. Merah, Design and instrumentation of force feedback in telerobotics, IEEE Trans. Instrum. Meas. 58 (6) (2008) 1949–1957, https://doi.org/10.1109/TIM.2008.2005858.

[17] J.Y. Chen, E.C. Haas, M.J. Barnes, Human performance issues and user interface design for teleoperated robots, IEEE Trans. Syst. Man Cybern. Part C Appl. Rev. 37 (6) (2007) 1231–1245, https://doi.org/10.1109/TSMCC.2007.905819.

[18] H. Boessenkool, et al., Analysis of human-in-the-loop tele-operated maintenance inspection tasks using VR, Fusion Eng. Design 88 (9–10) (2013) 2164–2167, https://doi.org/10.1016/j.fusengdes.2013.02.064.

[19] E.-L. Sallnäs, K. Rassmus-Gröhn, C. Sjöström, Supporting presence in collaborative environments by haptic force feedback, ACM Trans. Comp. Human Interact. (TOCHI) 7 (4) (2000) 461–476, https://doi.org/10.1145/365058.365086.

[20] I. Farkhatdinov, J.-H. Ryu, J. An, A preliminary experimental study on haptic teleoperation of mobile robot with variable force feedback gain, in: 2010 IEEE Haptics Symposium, IEEE, 2010, pp. 251–256, https://doi.org/10.1109/HAPTIC.2010.5444649.

[21] T.M. Lam, V. D'Amelio, M. Mulder, M. Van Paassen, UAV tele-operation using haptics with a degraded visual interface, in: 2006 IEEE International Conference on Systems, Man and Cybernetics 3, IEEE, 2006, pp. 2440–2445, https://doi.org/10.1109/ICSMC.2006.385229.

[22] G. Pegman, P. Desbats, F. Geffard, G. Piolain, A. Coudray, Force-Feedback Teleoperation of an Industrial Robot in a Nuclear Spent Fuel Reprocessing Plant, An International Journal, Industrial Robot, 2006, https://doi.org/10.1108/0143991061070300.

[23] A. Bolopion, S. Régnier, A review of haptic feedback teleoperation systems for micromanipulation and microassembly, IEEE Trans. Autom. Sci. Eng. 10 (3) (2013) 496–502, https://doi.org/10.1109/TASE.2013.2245122.

[24] T. Tsuji, K. Natori, H. Nishi, K. Ohnishi, A controller design method of bilateral control system, EPE J. 16 (2) (2006) 22–28, https://doi.org/10.1080/09398368.2006.11463616.

[25] S.M. Rahman, R. Ikeura, Weight-prediction-based predictive optimal position and force controls of a power assist robotic system for object manipulation, IEEE Trans. Ind. Electron. 63 (9) (2016) 5964–5975, https://doi.org/10.1109/TIE.2016.2561879.

[26] P. Pitakwatchara, S.-i. Warisawa, M. Mitsuishi, Analysis of the surgery task for the force feedback amplification in the minimally invasive surgical system, in: 2006 International Conference of the IEEE Engineering in Medicine and Biology Society, IEEE, 2006, pp. 829–832, https://doi.org/10.1109/IEMBS.2006.259933.

[27] F. Shah, A Telerobotic Drilling Control System with Haptic Feedback, Available: https://ir.lib.uwo.ca/etd/857, 2012.

[28] A. Shukla, H. Karki, Application of robotics in onshore oil and gas industry—a review part I, Robot. Auton. Syst. 75 (2016) 490–507, https://doi.org/10.1016/j.robot.2015.09.012.

[29] M.A. Goodrich, D.R. Olsen, J.W. Crandall, T.J. Palmer, Experiments in adjustable autonomy, in: Proceedings of IJCAI Workshop on autonomy, delegation and control: interacting with intelligent agents, 2001, pp. 1624–1629. Seattle, WA Available: http://ritter.ist.psu.edu/misc/dirk-files/papers/hri-papers/Experiments%20in%20Adjustable%20Autonomy.pdf.

[30] T.B. Sheridan, Teleoperation, telerobotics and telepresence: a progress report, Control. Eng. Pract. 3 (2) (1995) 205–214, https://doi.org/10.1016/0967-0661(94)00078-U.

[32] D.J. Bruemmer, D.D. Dudenhoeffer, J.L. Marble, Dynamic-autonomy for Urban search and rescue, in: AAAI Mobile Robot Competition, 2002, pp. 33–37. Available: https://www.aaai.org/Papers/Workshops/2002/WS-02-18/WS02-18-006.pdf.

[33] E. Krotkov, R. Simmons, F. Cozman, S. Koenig, Safeguarded teleoperation for lunar rovers: From human factors to field trials, IEEE Planet. Rover Technol. Syst. Workshop 26 (28) (1996) 92–99. Available: https://www.ri.cmu.edu/pub_files/pub1/krotkov_eric_1996_1/krotkov_eric_1996_1.pdf.

[34] C.W. Nielsen, M.A. Goodrich, R.W. Ricks, Ecological interfaces for improving mobile robot teleoperation, IEEE Trans. Robot. 23 (5) (2007) 927–941, https://doi.org/10.1109/TRO.2007.907479.

[35] A.E. Leeper, K. Hsiao, M. Ciocarlie, L. Takayama, D. Gossow, Strategies for human-in-the-loop robotic grasping, in: Proceedings of the seventh annual ACM/IEEE international conference on Human-Robot Interaction, 2012, pp. 1–8, https://doi.org/10.1145/2157689.2157691.

[36] A. Ajoudani, A.M. Zanchettin, S. Ivaldi, A. Albu-Schäffer, K. Kosuge, O. Khatib, Progress and prospects of the human–robot collaboration, Auton. Robot. 42 (5) (2018) 957–975, https://doi.org/10.1007/s10514-017-9677-2.

[37] G. Hoffman, C. Breazeal, Collaboration in human-robot teams, in: AIAA 1st Intelligent Systems Technical Conference, 2004, p. 6434, https://doi.org/10.2514/6.2004–6434.

[38] L.F. Penin, K. Matsumoto, Teleoperation with time delay: A survey and its use in space robotics, in: National Aerospace Laboratory (NAL), 2002, pp. 0389–4010. http://robotics.estec.esa.int/ASTRA/Astra2000/Papers/3.5b-4.PDF.

[39] S. Hirche, B. Stanczyk, M. Buss, Transparent exploration of remote environments by internet telepresence, in: Proceedings of Int. Workshop on High-Fidelity Telepresence and Teleaction jointly with the conference HUMANOIDS, 2003. Available: https://www.semanticscholar.org/paper/Transparent-Exploration-of-Remote-Environments-by-Hirche-Stanczyk/c5e1802c64029b0277f43c56e929a42ad187b3db?p2df.

[40] G.S. Guthart, J.K. Salisbury, The Intuitive/sup TM/telesurgery system: overview and application, in: Proceedings 2000 ICRA. Millennium Conference. IEEE International Conference on Robotics and Automation. Symposia Proceedings (Cat. No. 00CH37065) 1, IEEE, 2000, pp. 618–621, https://doi.org/10.1109/ROBOT.2000.844121.

[41] G. Guthart, J. Salisburg, The intuitive telesurgery system: overview and application, in: W: Proceedings of 2000 IEEE International Conference; 2000, on Robots and Automation. San Francisco, 22–28 April 2000, ed: IEEE, 2000.

[42] C.E. Lathan, M. Tracey, The effects of operator spatial perception and sensory feedback on human-robot teleoperation performance, Presence Teleoperat. Virtual Environm. 11 (4) (2002) 368–377, https://doi.org/10.1162/105474602760204282.

[43] S.J. Lederman, R.L. Klatzky, Haptic perception: A tutorial, Attent. Percept. Psychophys. 71 (7) (2009) 1439–1459, https://doi.org/10.3758/APP.71.7.1439.

[44] H. Tanaka, et al., Implementation of bilateral control system based on acceleration control using FPGA for multi-DOF haptic endoscopic surgery robot, IEEE Trans. Ind. Electron. 56 (3) (2008) 618–627, https://doi.org/10.1109/TIE.2008.2005710.

[45] B. Hannaford, A design framework for teleoperators with kinesthetic feedback, IEEE Trans. Robot. Autom. 5 (4) (1989) 426–434, https://doi.org/10.1109/70.88057.

[46] J. Park, O. Khatib, A haptic teleoperation approach based on contact force control, Int. J. Rob. Res. 25 (5–6) (2006) 575–591, https://doi.org/10.1177/0278364906065385.

[47] D. Lee, A. Franchi, H.I. Son, C. Ha, H.H. Bülthoff, P.R. Giordano, Semiautonomous haptic teleoperation control architecture of multiple unmanned aerial vehicles, IEEE/ASME Trans. Mech. 18 (4) (2013) 1334–1345, https://doi.org/10.1109/TMECH.2013.2263963.

[48] H.I. Son, et al., Measuring an operator's maneuverability performance in the haptic teleoperation of multiple robots, in: 2011 IEEE/RSJ International Conference on Intelligent Robots and Systems, IEEE, 2011, pp. 3039–3046, https://doi.org/10.1109/IROS.2011.6094618.

[49] T. Shimono, S. Katsura, K. Ohnishi, Abstraction and reproduction of force sensation from real environment by bilateral control, IEEE Trans. Ind. Electron. 54 (2) (2007) 907–918, https://doi.org/10.1109/TIE.2007.892744.

[50] H. Kobayashi, S. Katsura, K. Ohnishi, An analysis of parameter variations of disturbance observer for motion control, IEEE Trans. Ind. Electron. 54 (6) (2007) 3413–3421, https://doi.org/10.1109/TIE.2007.905948.

[51] K. Ohnishi, S. Katsura, T. Shimono, Motion control for real-world haptics, IEEE Ind. Electron. Mag. 4 (2) (2010) 16–19, https://doi.org/10.1109/MIE.2010.936761.

[52] TIAGo, TIAGo Mobile Manipulator, Available: http://www.tiago.pal-robotics.com, 2016.

[53] Ridgeback, Ridgeback: Omnidirectional Platform 2015, 2015. Available: http://www.clearpathrobotics.com/ridgeback/.

[54] Baxter, Baxter Research Robot, Available: http://www.rethinkrobotics.com/baxter-research-robot/, 2012.

[55] F.A. Freight, Fetch and Freight, Available: http://fetchrobotics.com/fetchandfreight/, 2014.

[56] Robotnik, Mobile Manipulators for Industry: The Future is Now, Available: https://www.robotnik.eu/manipulators-for-industry/, 2018.

[57] O. Khatib, K. Yokoi, K. Chang, D. Ruspini, R. Holmberg, A. Casal, Coordination and decentralized cooperation of multiple mobile manipulators, J. Robot. Syst. 13 (11) (1996) 755–764, https://doi.org/10.1002/(SICI)1097-4563(199611)13:11<755::AID-ROB6>3.0.CO;2-U.

[58] J.E. Naranjo, E.C. Lozada, H.I. Espín, C. Beltran, C.A. García, M.V. García, Flexible architecture for transparency of a bilateral tele-operation system implemented in mobile anthropomorphic robots for the oil and gas industry, IFAC-PapersOnLine 51 (8) (2018) 239–244, https://doi.org/10.1016/j.ifacol.2018.06.383.

[59] D.G. Lee, G.R. Cho, M.S. Lee, B.-S. Kim, S. Oh, H.I. Son, Human-centered evaluation of multi-user teleoperation for mobile manipulator in unmanned offshore plants, in: 2013 IEEE/RSJ International Conference on Intelligent Robots and Systems, IEEE, 2013, pp. 5431–5438, https://doi.org/10.1109/IROS.2013.6697142.

[60] R.O. Faria, et al., A methodology for autonomous robotic manipulation of valves using visual sensing, IFAC-PapersOnLine 48 (6) (2015) 221–228, https://doi.org/10.1016/j.ifacol.2015.08.035.

[61] D.A. Anisi, J. Gunnar, T. Lillehagen, C. Skourup, Robot automation in oil and gas facilities: Indoor and onsite demonstrations, in: 2010 IEEE/RSJ International Conference on Intelligent Robots and Systems, IEEE, 2010, pp. 4729–4734, https://doi.org/10.1109/IROS.2010.5649281.

[62] M.A. Roa, D. Berenson, W. Huang, Mobile manipulation: toward smart manufacturing [tc spotlight], IEEE Rob. Autom. Magaz. 22 (4) (2015) 14–15, https://doi.org/10.1109/MRA.2015.2486583.

[63] H. Seraji, A unified approach to motion control of mobile manipulators, Int. J. Rob. Res. 17 (2) (1998) 107–118, https://doi.org/10.1177/027836499801700201.

[64] Y. Yamamoto, X. Yun, Effect of the dynamic interaction on coordinated control of mobile manipulators, IEEE Trans. Robot. Autom. 12 (5) (1996) 816–824, https://doi.org/10.1109/70.538986.

[65] J. Vannoy, J. Xiao, Real-time adaptive motion planning (RAMP) of mobile manipulators in dynamic environments with unforeseen changes, IEEE Trans. Robot. 24 (5) (2008) 1199–1212, https://doi.org/10.1109/TRO.2008.2003277.

[66] R.B. Rusu, A. Holzbach, R. Diankov, G. Bradski, M. Beetz, Perception for mobile manipulation and grasping using active stereo, in: 2009 9th IEEE-RAS International Conference on Humanoid Robots, IEEE, 2009, pp. 632–638, https://doi.org/10.1109/ICHR.2009.5379597.

[67] S. Chitta, E.G. Jones, M. Ciocarlie, K. Hsiao, Perception, planning, and execution for mobile manipulation in unstructured environments, IEEE Rob. Autom. Magaz. Spec. Issue Mob. Manipul. 19 (2) (2012) 58–71. Available: http://1.willowgarage.org/sites/default/files/chitta_ram_2011.pdf.

[68] C. Bartneck, D. Kulić, E. Croft, S. Zoghbi, Measurement instruments for the anthropomorphism, animacy, likeability, perceived intelligence, and perceived safety of robots, Int. J. Soc. Robot. 1 (1) (2009) 71–81, https://doi.org/10.1007/s12369-008-0001-3.

[70] Z. Li, S.S. Ge, M. Adams, W.S. Wijesoma, Robust adaptive control of uncertain force/motion constrained nonholonomic mobile manipulators, Automatica 44 (3) (2008) 776–784, https://doi.org/10.1016/j.automatica.2007.07.012.

[71] B.S. Bloom, Taxonomy of Educational Objectives. Vol. 1: Cognitive Domain, McKay, New York, 1956, pp. 20–24. Available: http://nancybroz.com/nancybroz/Literacy_I_files/Bloom%20Intro.doc.

[72] J.V. Nickerson, S.S. Skiena, Attention and communication: Decision scenarios for teleoperating robots, in: Proceedings of the 38th Annual Hawaii International Conference on System Sciences, IEEE, 2005, p. 295c, https://doi.org/10.1109/HICSS.2005.107.

[73] T. Carlson, Y. Demiris, Collaborative control for a robotic wheelchair: evaluation of performance, attention, and workload, IEEE Trans. Syst. Man Cybern. Part B (Cybern.) 42 (3) (2012) 876–888, https://doi.org/10.1109/TSMCB.2011.2181833.

[74] T. Carlson, Y. Demiris, Using visual attention to evaluate collaborative control architectures for human robot interaction, in: Proceedings of New Frontiers in Human-Robot Interaction: A symposium at the AISB 2009 Convention, SSAISB, 2009, pp. 38–43, no. CONF. Available: https://infoscience.epfl.ch/record/150462/.

[75] Y. Shi, J. Du, E. Ragan, Review visual attention and spatial memory in building inspection: toward a cognition-driven information system, Adv. Eng. Inform. 44 (2020) 101061, https://doi.org/10.1016/j.aei.2020.101061.

[76] G.E. Raptis, C.A. Fidas, N.M. Avouris, Using eye tracking to identify cognitive differences: A brief literature review, in: Proceedings of the 20th Pan-Hellenic Conference on Informatics, 2016, pp. 1–6, https://doi.org/10.1145/3003733.3003762.

[77] Y. Shi, J. Du, S.P. Sargunam, E.D. Ragan, Q. Zhu, First responders' spatial working memory of large-scale buildings: implications of information format, in: Presented at the Computing in Civil Engineering 2019: Visualization, Information Modeling, and Simulation, 2019, https://doi.org/10.1061/9780784482421.020.

[78] Y. Shi, J. Du, Simulation of spatial memory for human navigation based on visual attention in floorplan review, in: 2019 Winter Simulation Conference (WSC), IEEE, 2019, pp. 3031–3040, https://doi.org/10.1109/WSC40007.2019.9004783.

[80] J.M. Henderson, A. Hollingworth, Eye movements during scene viewing: An overview, in: Eye Guidance in Reading and Scene Perception, Elsevier, 1998, pp. 269–293, https://doi.org/10.1016/B978-008043361-5/50013-4.

[81] Y. Shi, Y. Zhu, R.K. Mehta, J. Du, A neurophysiological approach to assess training outcome under stress: a virtual reality experiment of industrial shutdown maintenance using functional near-infrared spectroscopy (fNIRS), Adv. Eng. Inform. 46 (2020) 101153.

[82] S.C. Bunce, M. Izzetoglu, K. Izzetoglu, B. Onaral, K. Pourrezaei, Functional near-infrared spectroscopy, IEEE Eng. Med. Biol. Magazine 25 (4) (2006) 54–62, https://doi.org/10.1109/MEMB.2006.1657788.

[83] J. Du, Q. Zhu, Y. Shi, Q. Wang, Y. Lin, D. Zhao, Cognition digital twins for personalized information systems of smart cities: Proof of concept, J. Manag. Eng. 36 (2) (2020) 04019052, https://doi.org/10.1061/(ASCE)ME.1943-5479.0000740.

[84] P. Pinti, et al., The Present and Future Use of Functional near-Infrared Spectroscopy (fNIRS) for Cognitive Neuroscience, Annals of the New York Academy of Sciences, 2018, https://doi.org/10.1111/nyas.13948.

[85] K.N. Ochsner, S.A. Bunge, J.J. Gross, J.D. Gabrieli, Rethinking feelings: an FMRI study of the cognitive regulation of emotion, J. Cogn. Neurosci. 14 (8) (2002) 1215–1229, https://doi.org/10.1162/089892902760807212.

[86] N.C. Andreasen, et al., Schizophrenia and cognitive dysmetria: a positron-emission tomography study of dysfunctional prefrontal-thalamic-cerebellar circuitry, Proc. Natl. Acad. Sci. 93 (18) (1996) 9985–9990, https://doi.org/10.1073/pnas.93.18.9985.

[87] W.J. Ray, H.W. Cole, EEG alpha activity reflects attentional demands, and beta activity reflects emotional and cognitive processes, Science 228 (4700) (1985) 750–752, https://doi.org/10.1126/science.3992243.

[88] E. Halgren, T. Raij, K. Marinkovic, V. Jousmäki, R. Hari, Cognitive response profile of the human fusiform face area as determined by MEG, Cereb. Cortex 10 (1) (2000) 69–81, https://doi.org/10.1093/cercor/10.1.69.

[89] C. Herff, D. Heger, O. Fortmann, J. Hennrich, F. Putze, T. Schultz, Mental workload during n-back task—quantified in the prefrontal cortex using fNIRS, Front. Hum. Neurosci. 7 (2014) 935, https://doi.org/10.3389/fnhum.2013.00935.

[90] N. Ramnani, A.M. Owen, Anterior prefrontal cortex: insights into function from anatomy and neuroimaging, Nat. Rev. Neurosci. 5 (3) (2004) 184–194, https://doi.org/10.1038/nrn1343.

[91] D.R. Leff, et al., Assessment of the cerebral cortex during motor task behaviours in adults: a systematic review of functional near infrared spectroscopy (fNIRS) studies, Neuroimage 54 (4) (2011) 2922–2936, https://doi.org/10.1016/j.neuroimage.2010.10.058.

[92] Y. Shi, J. Du, C.R. Ahn, E. Ragan, Impact assessment of reinforced learning methods on construction workers' fall risk behavior using virtual reality, Autom. Constr. 104 (2019) 197–214, https://doi.org/10.1016/j.autcon.2019.04.015.

[93] Q. Zhu, J. Du, Y. Shi, Q. Wang, Y. Lin, Participatory and evolutionary fire simulation via a sensitive control of key scenery parameters, in: Computing in Civil Engineering 2019: Visualization, Information Modeling, and Simulation, American Society of Civil Engineers Reston, VA, 2019, pp. 103–111, https://doi.org/10.1061/9780784482421.014.

[94] J. Du, Q. Wang, Y. Lin, C. Ahn, Personalize wayfinding information for fire responders based on virtual reality training data, in: Proceedings of the 52nd Hawaii International Conference on System Sciences, 2019, https://doi.org/10.24251/HICSS.2019.240.

[95] J. Du, Y. Shi, Z. Zou, D. Zhao, CoVR: Cloud-based multiuser virtual reality headset system for project communication of remote users, J. Constr. Eng. Manag. 144 (2) (2018) 04017109, https://doi.org/10.1061/(ASCE)CO.1943-7862.0001426.

[96] J. Du, Z. Zou, Y. Shi, D. Zhao, Zero latency: real-time synchronization of BIM data in virtual reality for collaborative decision-making, Autom. Constr. 85 (2018) 51–64, https://doi.org/10.1016/j.autcon.2017.10.009.

[97] J. Du, Z. Zou, Y. Shi, D. Zhao, Simultaneous data exchange between BIM and VR for collaborative decision making, in: Computing in Civil Engineering 2017, 2017, pp. 1–8, https://doi.org/10.1061/9780784480830.001.

[98] J. Du, Y. Shi, C. Mei, J. Quarles, W. Yan, Communication by interaction: A multiplayer VR environment for building walkthroughs, in: Construction Research Congress 2016, 2016, pp. 2281–2290, https://doi.org/10.1061/9780784479827.227.

[99] S. Martin, N. Hillier, Characterisation of the Novint Falcon haptic device for application as a robot manipulator, in: Australasian Conference on Robotics and Automation (ACRA), Citeseer, 2009, pp. 291–292. Available: http://citeseerx.ist.psu.edu/viewdoc/download?doi=10.1.1.368.6007&rep=rep1&type=pdf.

[100] O. Linda, M. Manic, Self-organizing fuzzy haptic teleoperation of mobile robot using sparse sonar data, IEEE Trans. Ind. Electron. 58 (8) (2009) 3187–3195, https://doi.org/10.1109/TIE.2009.2037649.

[101] J. Feiling, Z. Li, H. Yu, H. Ren, Optimal teleoperation control of a constrained tendon-driven serpentine manipulator, in: 2015 IEEE 28th Canadian Conference on Electrical and Computer Engineering (CCECE), IEEE, 2015, pp. 418–423, https://doi.org/10.1109/CCECE.2015.7129314.

[102] P. Chotiprayanakul, D. Liu, Workspace mapping and force control for small haptic device based robot teleoperation, in: 2009 International Conference on Information and Automation, IEEE, 2009, pp. 1613–1618, https://doi.org/10.1109/ICINFA.2009.5205175.

[103] S.R. Ellis, K. Mania, B.D. Adelstein, M.I. Hill, Generalizeability of latency detection in a variety of virtual environments, in: Proceedings of the Human Factors and Ergonomics Society Annual Meeting 48, SAGE Publications Sage CA, Los Angeles, CA, 2004, pp. 2632–2636, https://doi.org/10.1177/154193120404802306, no. 23.

[104] J.C. Lane, C.R. Carignan, B.R. Sullivan, D.L. Akin, T. Hunt, R. Cohen, Effects of time delay on telerobotic control of neutral buoyancy vehicles, in: Proceedings 2002 IEEE International Conference on Robotics and Automation (Cat. No. 02CH37292) 3, IEEE, 2002, pp. 2874–2879, https://doi.org/10.1109/ROBOT.2002.1013668.

[105] R.B. Ekstrom, D. Dermen, H.H. Harman, Manual for Kit of Factor-Referenced Cognitive Tests, Educational testing service Princeton, NJ, 1976. Available: https://www.ets.org/Media/Research/pdf/Manual_for_Kit_of_Factor-Referenced_Cognitive_Tests.pdf.

[106] S.G. Hart, L.E. Staveland, Development of NASA-TLX (Task Load Index): Results of empirical and theoretical research, in: (Eds.), Advances in Psychology 52, Elsevier, 1988, p. 139, https://doi.org/10.1016/S0166-4115(08)62386-9.

[107] B.R. Manor, E. Gordon, Defining the temporal threshold for ocular fixation in free-viewing visuocognitive tasks, J. Neurosci. Methods 128 (1–2) (2003) 85–93, https://doi.org/10.1016/S0165-0270(03)00151-1.

[108] P. Pinti, F. Scholkmann, A. Hamilton, P. Burgess, I. Tachtsidis, Current status and issues regarding pre-processing of fNIRS neuroimaging data: An investigation of diverse signal filtering methods within a general linear model framework, Front. Hum. Neurosci. 12 (2018) 505, https://doi.org/10.3389/fnhum.2018.00505.

[109] T.J. Huppert, S.G. Diamond, M.A. Franceschini, D.A. Boas, HomER: a review of time-series analysis methods for near-infrared spectroscopy of the brain, Appl. Opt. 48 (10) (2009) D280–D298, https://doi.org/10.1364/AO.48.00D280.

[110] M. Peña, et al., Sounds and silence: an optical topography study of language recognition at birth, Proc. Natl. Acad. Sci. 100 (20) (2003) 11702–11705, https://doi.org/10.1073/pnas.1934290100.

[111] D.T. Delpy, M. Cope, P. van der Zee, S. Arridge, S. Wray, J. Wyatt, Estimation of optical pathlength through tissue from direct time of flight measurement, Phys. Med. Biol. 33 (12) (1988) 1433. Available: https://iopscience.iop.org/article/10.1088/0031-9155/33/12/008/meta?casa_token=a_LsmzqoagUAAAAA:e2D3gWf10pNDMTQnZRUVKkadLRzAc85-tI0pYFhr-2vyULeNA7EXt5qARxs7shtod2PWL5fXN5Y.

[112] Y. Hoshi, N. Kobayashi, M. Tamura, Interpretation of near-infrared spectroscopy signals: a study with a newly developed perfused rat brain model, J. Appl. Physiol. 90 (5) (2001) 1657–1662, https://doi.org/10.1152/jappl.2001.90.5.1657.

[113] H. Ayaz, P.A. Shewokis, S. Bunce, K. Izzetoglu, B. Willems, B. Onaral, Optical brain monitoring for operator training and mental workload assessment, Neuroimage 59 (1) (2012) 36–47, https://doi.org/10.1016/j.neuroimage.2011.06.023.

[114] Z. Lin, G. Ma, B. Cui, Y. Li, Z. Zhu, N. Tong, Influence of flashboard location on flow resistance properties and internal features of gate valve under the variable condition, J. Nat. Gas Sci. Eng. 33 (2016) 108–117, https://doi.org/10.1016/j.jngse.2016.05.025.

[115] K. Refalo, S. Bowyer, M. Smith, M. Hijawi, Optimizing valve rotational speed using Taguchi techniques, in: SAE Technical Paper 0148–7191, 2010, https://doi.org/10.4271/2010-01-1096.

[116] C.-K. Kim, S.-M. Lee, C.-M. Jang, Performance analysis of a ball valve used for gas pipelines by introducing nondimensional parameters, Adv. Mech. Eng. 11 (1) (2019), https://doi.org/10.1177/1687814018823350, 1687814018823350.

[117] L.-C. Shi, Y.-Y. Jiao, B.-L. Lu, Differential entropy feature for EEG-based vigilance estimation, in: 2013 35th Annual International Conference of the IEEE Engineering in Medicine and Biology Society (EMBC), IEEE, 2013, pp. 6627–6630, https://doi.org/10.1109/EMBC.2013.6611075.

[118] D. Darmon, Specific differential entropy rate estimation for continuous-valued time series, Entropy 18 (5) (2016) 190, https://doi.org/10.3390/e18050190.

[119] R.-N. Duan, J.-Y. Zhu, B.-L. Lu, Differential entropy feature for EEG-based emotion classification, in: 2013 6th International IEEE/EMBS Conference on Neural Engineering (NER), IEEE, 2013, pp. 81–84, https://doi.org/10.1109/NER.2013.6695876.

[120] D. Rakita, B. Mutlu, M. Gleicher, Effects of onset latency and robot speed delays on mimicry-control teleoperation, in: HRI, 2020, pp. 519–527. Available: https://graphics.cs.wisc.edu/Papers/2020/RMG20/rmg-hri2020.pdf.

[121] G.R. Finney, Perceptual-motor dysfunction, Continuum: Lifelong Learn. Neurol. 21 (3) (2015) 678–689, https://doi.org/10.1212/01.CON.0000466660.82284.69.

[122] A.J. Ayres, Patterns of perceptual-motor dysfunction in children: A factor analytic study, Percept. Mot. Skills 20 (2) (1965) 335–368, https://doi.org/10.2466/pms.1965.20.2.335.

[123] M. Wallen, R. Walker, Occupational therapy practice with children with perceptual motor dysfunction: findings of a literature review and survey, Aust. Occup. Ther. J. 42 (1) (1995) 15–25, https://doi.org/10.1111/j.1440-1630.1995.tb01306.x.

[124] G. Wood, S.J. Vine, M.R. Wilson, The impact of visual illusions on perception, action planning, and motor performance, Attent. Percept. Psychophys. 75 (5) (2013) 830–834, https://doi.org/10.3758/s13414-013-0489-y.

[125] W. Kirsch, W. Kunde, Moving further moves things further away in visual perception: position-based movement planning affects distance judgments, Exp. Brain Res. 226 (3) (2013) 431–440, https://doi.org/10.1007/s00221-013-3455-y.

[126] M.N. Shadlen, W.T. Newsome, Motion perception: seeing and deciding, Proc. Natl. Acad. Sci. 93 (2) (1996) 628–633, https://doi.org/10.1073/pnas.93.2.628.

[127] A. Bauer, D. Wollherr, M. Buss, Human–robot collaboration: a survey, Int. J. Human. Rob. 5 (01) (2008) 47–66, https://doi.org/10.1142/S0219843608001303.

[128] W.S. Newman, Stability and Performance Limits of Interaction Controllers, 1992, https://doi.org/10.1115/1.2897725.

[129] S.P. Buerger, N. Hogan, Complementary stability and loop shaping for improved human–robot interaction, IEEE Trans. Robot. 23 (2) (2007) 232–244, https://doi.org/10.1109/TRO.2007.892229.
[130] K. Abidi, Y. Yildiz, B. Korpe, Explicit time-delay compensation in teleoperation: An adaptive control approach, Int. J. Rob. Nonlin. Control 26 (15) (2016) 3388–3403, https://doi.org/10.1002/rnc.3513.
[131] Z. Chen, Y.J. Pan, J. Gu, Integrated adaptive robust control for multilateral teleoperation systems under arbitrary time delays, Int. J. Rob. Nonlin. Control 26 (12) (2016) 2708–2728, https://doi.org/10.1002/rnc.3472.
[132] J. Burgner-Kahrs, D.C. Rucker, H. Choset, Continuum robots for medical applications: a survey, IEEE Trans. Robot. 31 (6) (2015) 1261–1280, https://doi.org/10.1109/TRO.2015.2489500.
[133] C. Yang, J. Luo, Y. Pan, Z. Liu, C.-Y. Su, Personalized variable gain control with tremor attenuation for robot teleoperation, IEEE Trans. Syst. Man Cybern. Syst. 48 (10) (2017) 1759–1770, https://doi.org/10.1109/TSMC.2017.2694020.